Advanced Topics on Modern Radar

Airborne radar

Airborne Radar

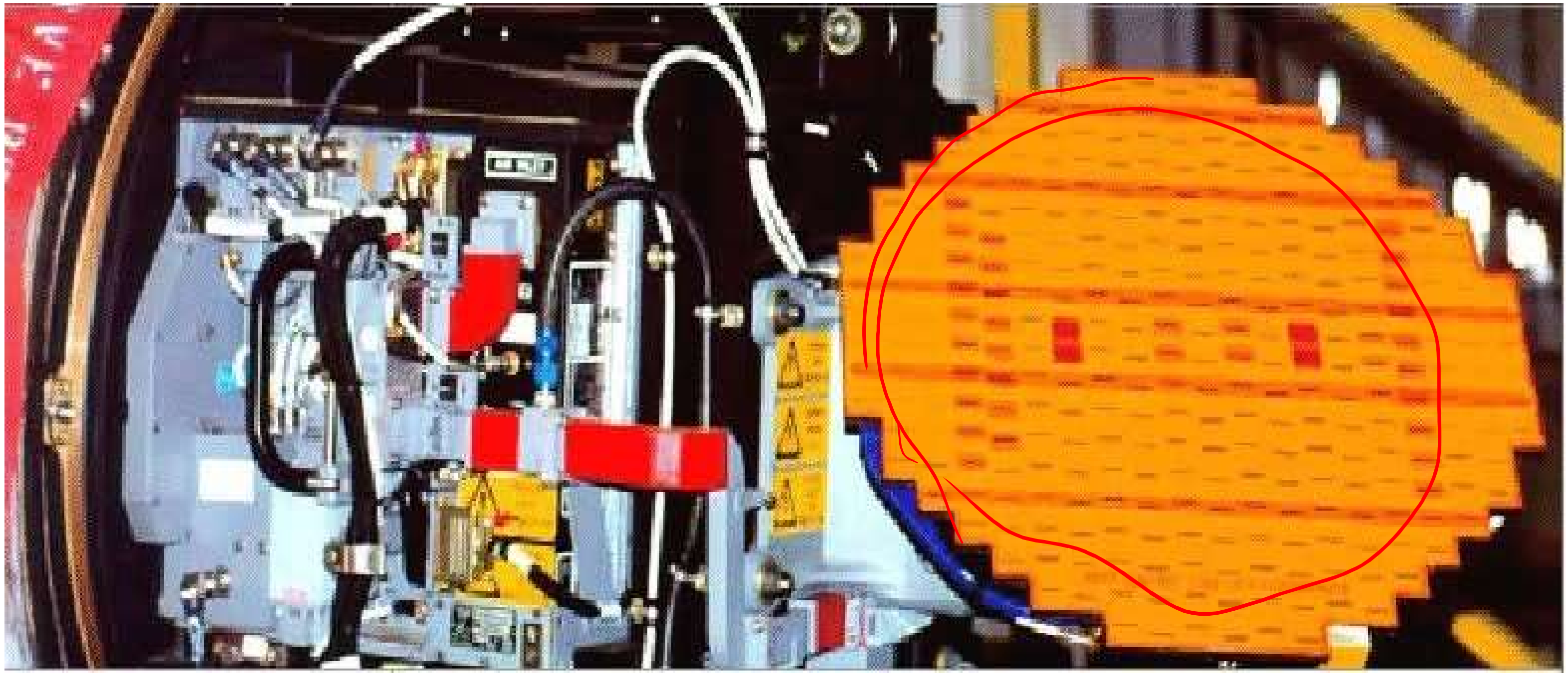

Leonardo - Finmeccanica

Radiation Pattern - Shape #6 not E 2 TX az

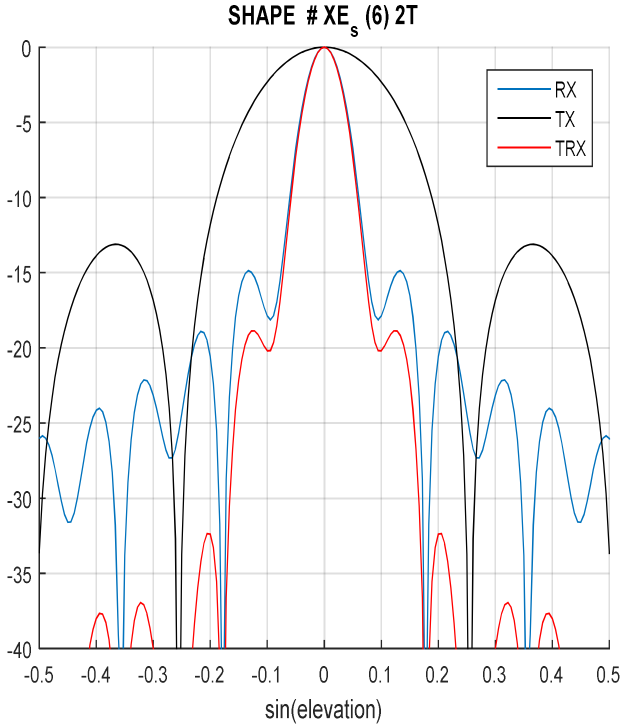

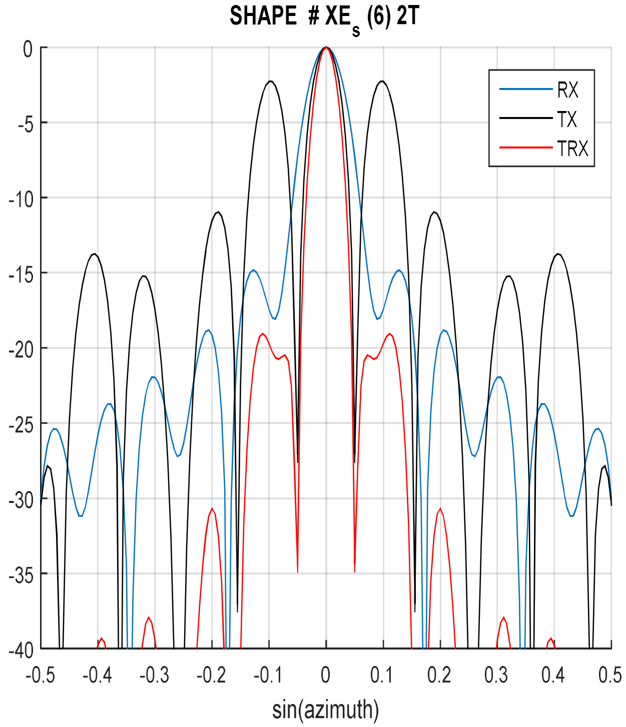

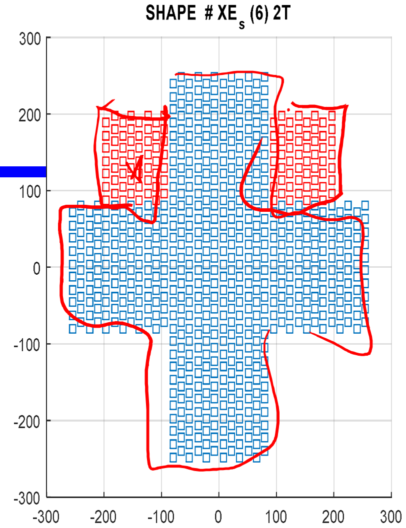

RX: $BW_{el} = 3.85°$ $SLL_{el} = -14.9\ dB$

RX: $BW_{az} = 3.70°$ $SLL_{az} = -14.8\ dB$

TRX: $BW_{el} = 3.70°$ $SLL_{el} = -18.9\ dB$

TRX: $BW_{az} = 2.29°$ $SLL_{az} = -19.1\ dB$

Array configuration - Shape #6 Estesa X2 – 3 TX vs #2

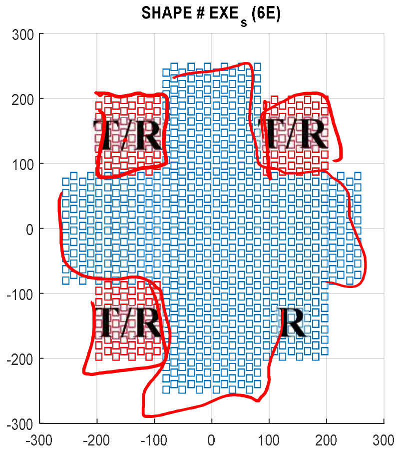

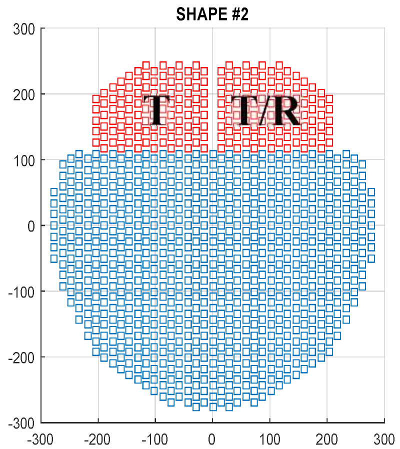

TRX	num. el. RX	num. el. TX	BW el [deg]	BW az [deg]	SLL el [dB]	SLL az [dB]	SLL tot [dB]
Shape Grifo-e	592	592	3.45	**2.45**	-28.5	-30.3	**-28.5**

Shape #6 TRX	num. el. RX	num. el. TX	BW el [deg]	BW az [deg]	SLL el [dB]	SLL az [dB]	SLL tot [dB]
2 E az 1 TX + com	600 + 112	56	3.58	**3.40**	-22.7	-24.8	**-17.0**
2 E az 2 TX az	600 + 112	112	3.58	**2.25**	-22.7	-25.7	**-18.5**

Shape #6 TRX	num. el. RX	num. el. TX	BW el [deg]	BW az [deg]	SLL el [dB]	SLL az [dB]	SLL tot [dB]
2 E az 1 TX + com	600 + 112	56	3.58	**3.40**	-22.7	-24.8	**-17.0**
4 E 1 TX	600 + 224	56	3.39	**3.30**	-20.9	-20.6	**-19.0**
4 E 2 TX az	600 + 224	112	3.39	**2.22**	-20.9	-20.9	**-20.9**

Shape #6 TRX	num. el. RX	num. el. TX	BW el [deg]	BW az [deg]	SLL el [dB]	SLL az [dB]	SLL tot [dB]
2 E az 2 TX az + com + esm	600 + 112	112	3.58	**2.25**	-22.7	-25.7	**-18.5**
2 E el 2 TX el + com + esm	600 + 112	112	2.25	**3.58**	-25.7	-22.7	**-18.5**
4 E 1 TX	600 + 224	56	3.39	**3.30**	-20.9	-20.6	**-19.0**
4 E 2 TX az	600 + 224	112	3.39	**2.22**	-20.9	-20.9	**-20.9**
4 E 2 TX el	600 + 224	112	2.22	**3.39**	-20.9	-20.9	**-20.9**

Shape #2 TRX	num. el. RX	num. el. TX	BW el [deg]	BW az [deg]	SLL el [dB]	SLL az [dB]	SLL tot [dB]
1 TX + com	762	103	4.01	**2.79**	-19.2	-20.9	**-19.2**
2 TX	762	206	4.01	**2.36**	-19.2	-32.3	**-19.2**

Shape 6 e 7

Shape #6 – Cross Even squared TX   Shape #7 – Cross Even rectangular TX

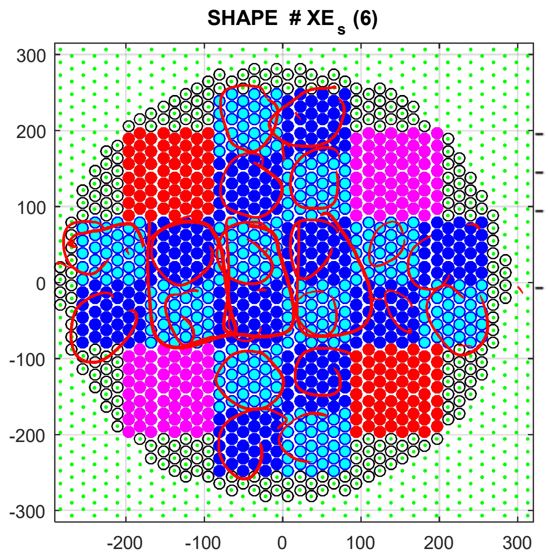

RX
- num elem: 600
- Nx: 36
- Ny: 30
- easy regular subarray division: (6x5)

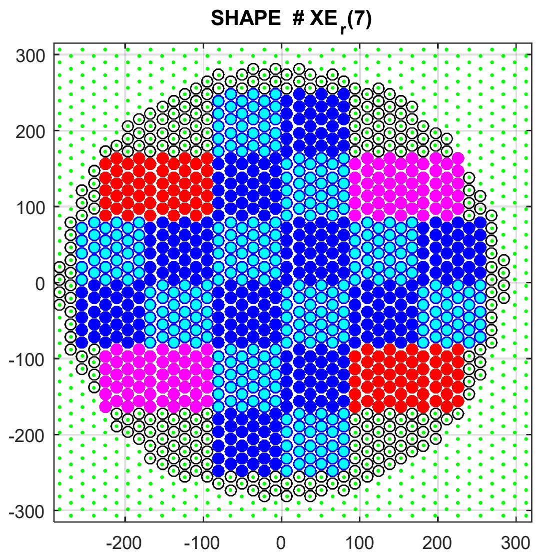

4 x TX
- num elem: 56 Nx: 8 Ny: 7

4 x TX
- num elem: 50 Nx: 10 Ny: 5

Motivation for MIMO n. 2 (cont'd)

1D & 2D Interference spectrum

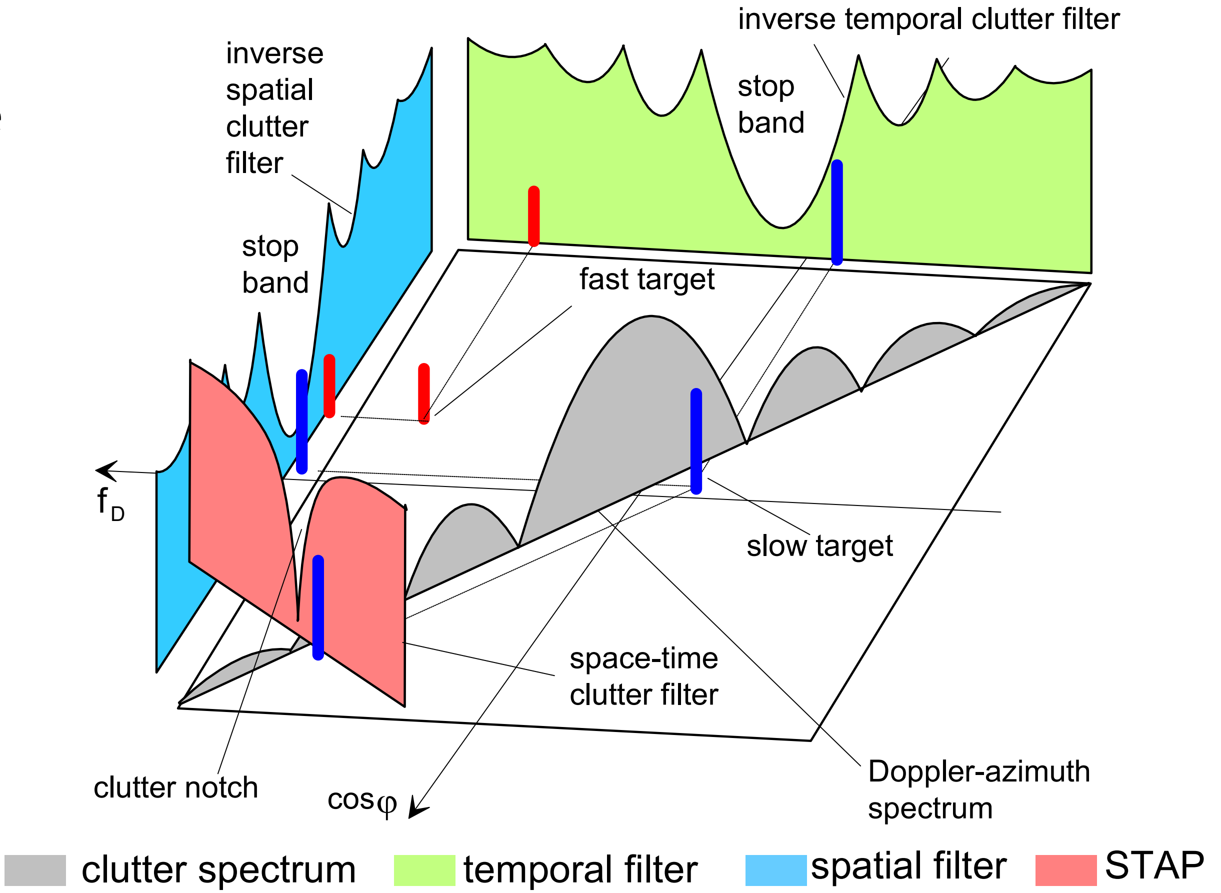

One dimensional temporal and spatial filters compared to the two-dimensional space-time filter (Reference: J. Ender; R. Klemm, IEE Radar 92). - **Superior performance of space-time processing for target detection.**

Motivation for MIMO n. 2 (cont'd)

- With N RX beams, max displacement between 2-way phase centers is (N-1) times the RXs spacing

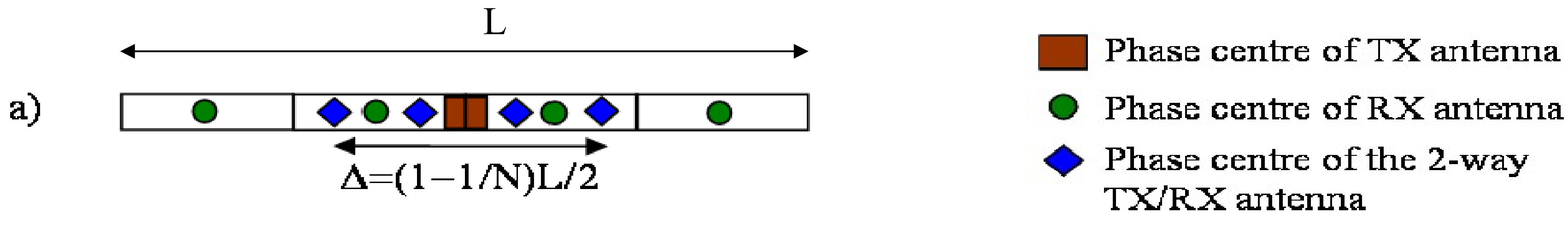

- Clutter notch width is inversely proportional to Δ

- Narrowest notch is filter like 1-beam at clutter $(1-\text{sinc}(\pi\Delta\sin(\varphi))$

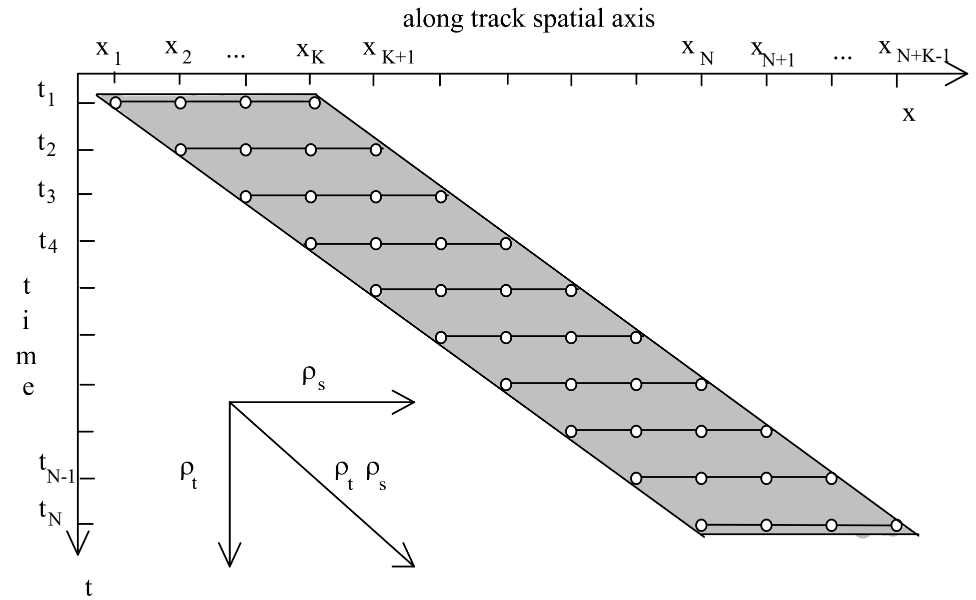

desired Maximum diplacement that allows to avoid sidelobes!

Forward-looking STAP

➢ **Elaborazione spazio-tempo:**

I segnali si propagano con onde che sono funzioni sia dello spazio che del tempo, allora si può fondere l'**elaborazione spaziale**, che equivale a sintetizzare un pattern d'antenna, con un **elaborazione temporale**, che su un radar ad impulsi si basa sulla possibilità di collezionare impulsi consecutivi, trasmessi ad una certa PRF

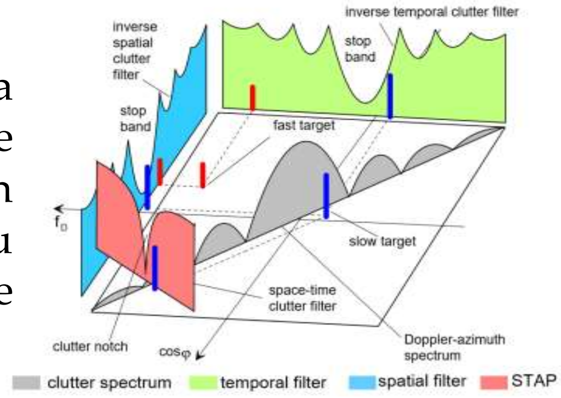

Configurazioni operative

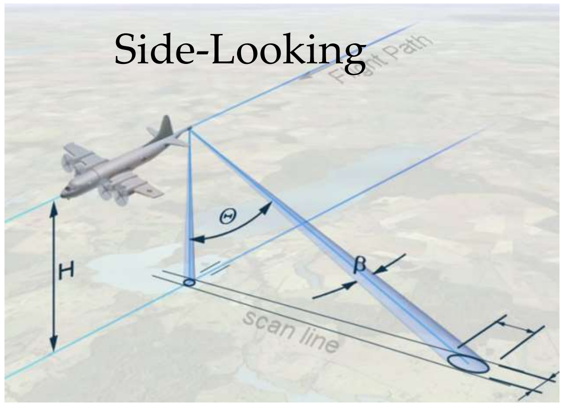

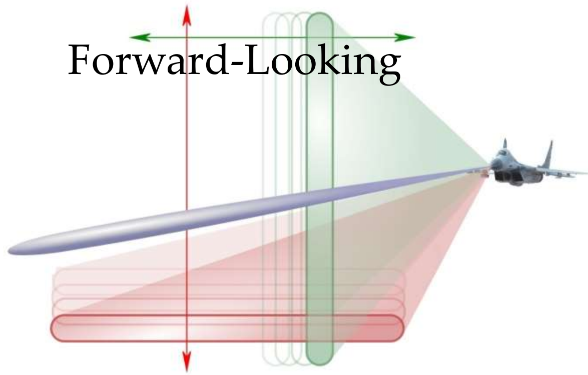

Passive Radar

EU Project - SPYGLASS

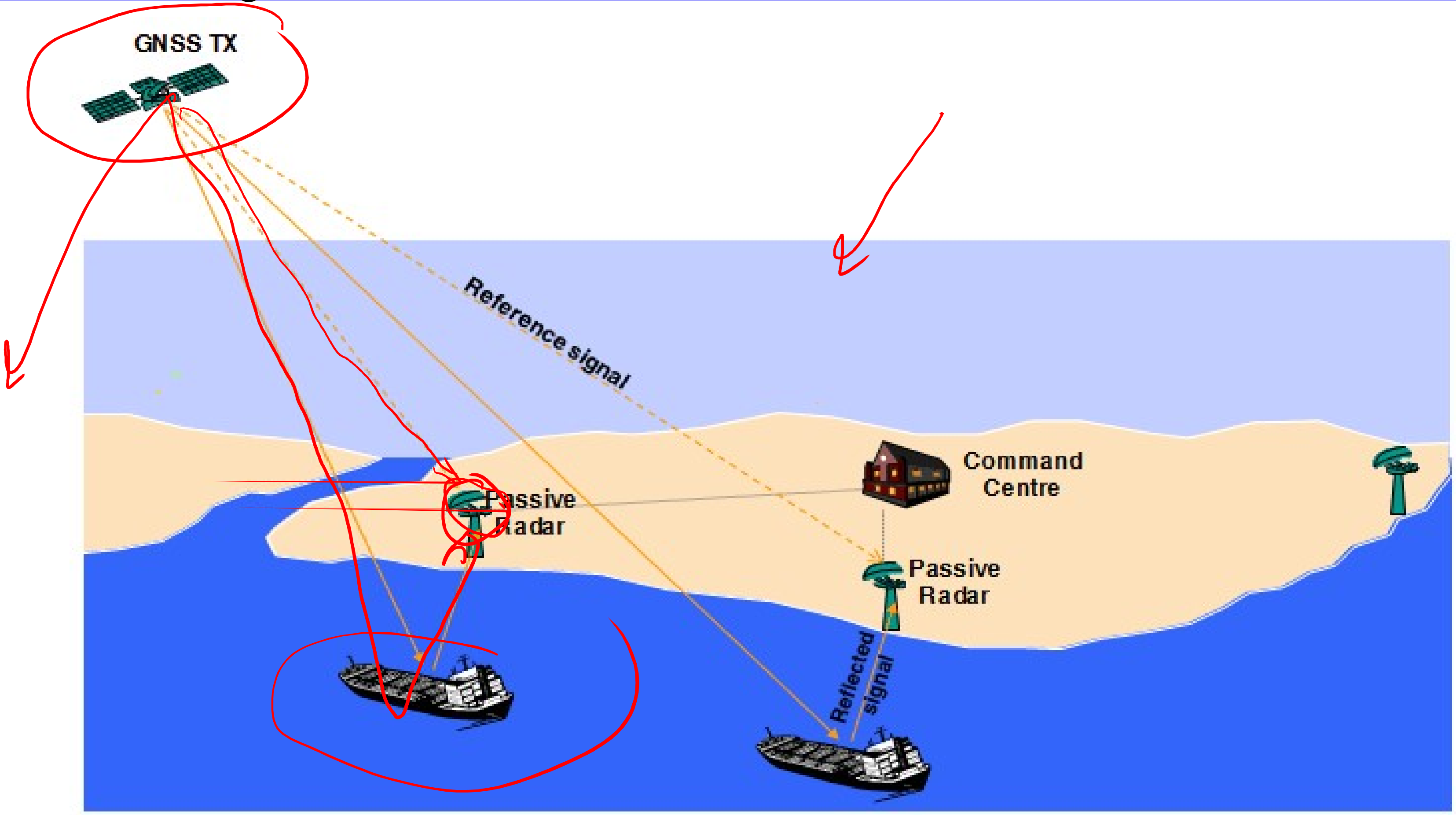

GALILEO-Based Passive Radar System for Maritime Surveillance

SPYGLASS Architecture

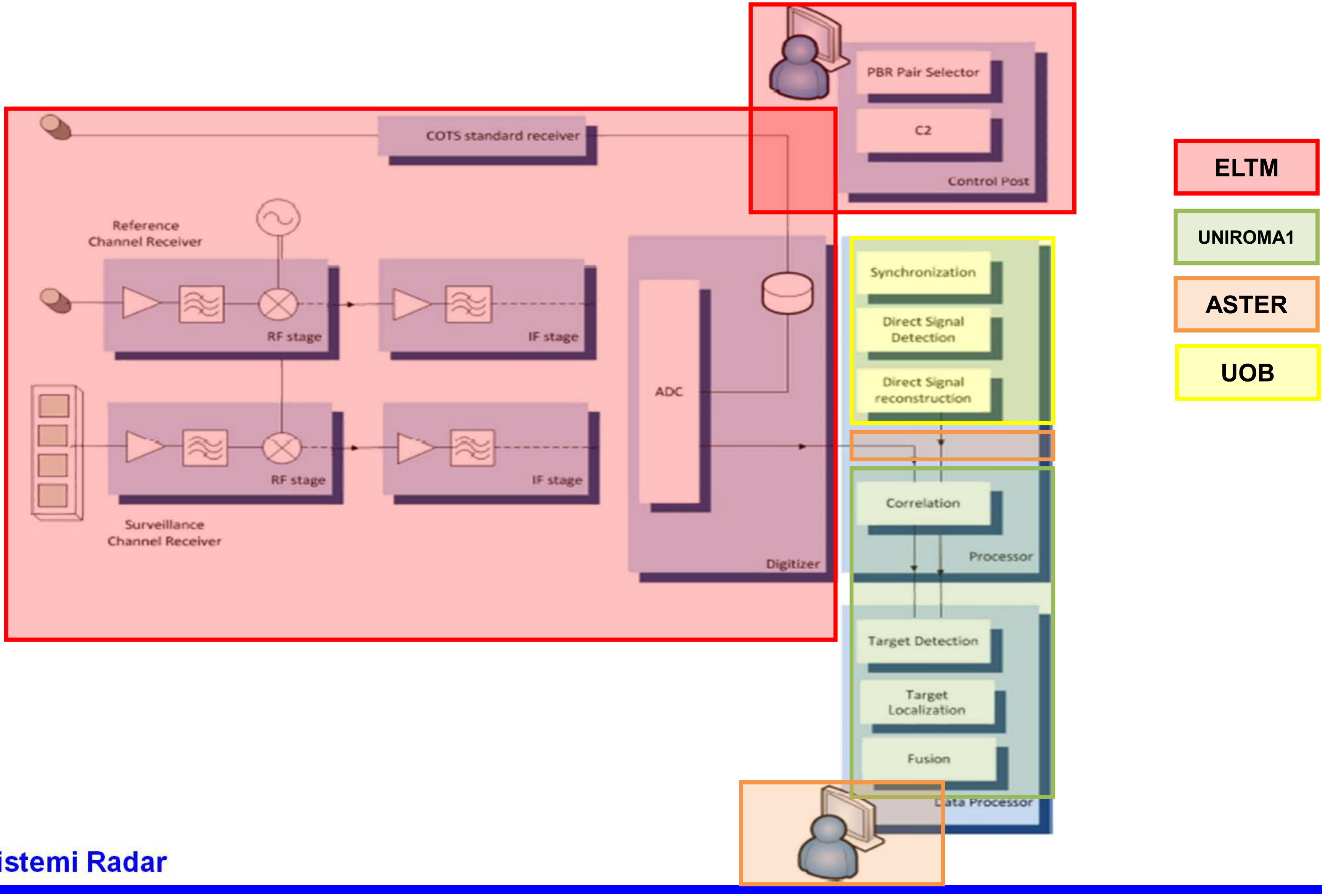

WP2 – Passive GNSS based M-MTI Mode

Objectives: Development of PBR processing techniques for maritime moving target detection

- Study, development and testing of processing techniques for maritime moving target detection and localization by means of PBR techniques exploiting GNSS as opportunity transmitters and ground-based or balloon-based receiving systems

- Definition of the required enabling techniques able to provide the Maritime-MTI (Moving Target Indication) capabilities

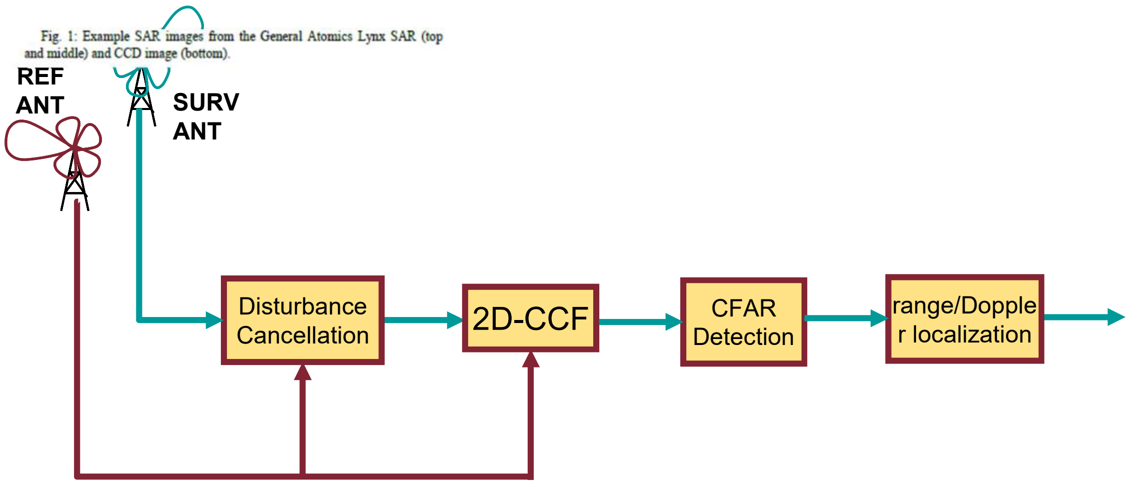

PBR for maritime applications

PBR advantages:

low cost, reduced impact on the environment, small size, rapid update.

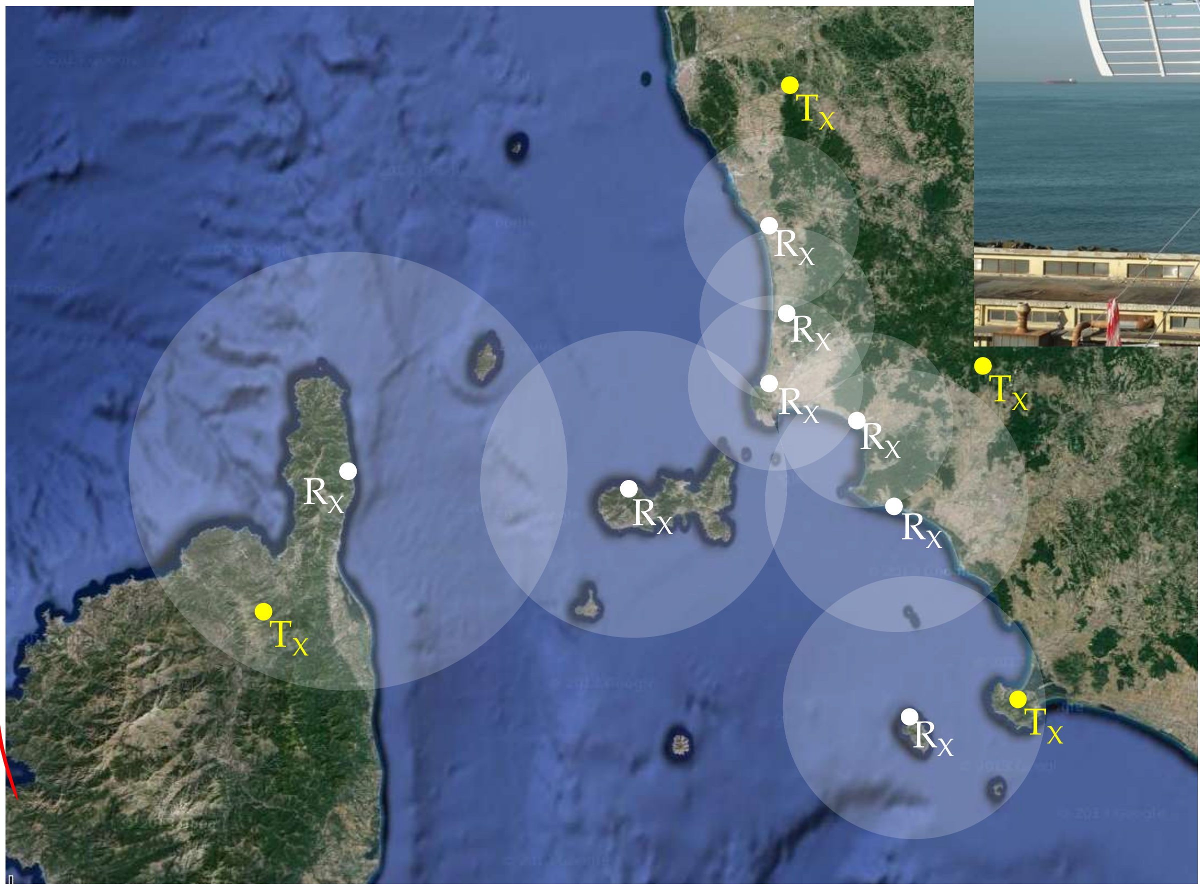

Could guarantee complete and continuous coverage

Could be used as Gap filler

SELEX - ES

DVB-T Signal Ambiguity Function Control

RESIDUAL PEAKS REMOVAL (RPR) FILTER

$$R_{eq}[l] = \chi_{eq}[l,0] = \sum_{n=0}^{N-1} s[n]\, s_{eq}^{*}[n-l]$$

DVB-T signal mismatched Auto-Correlation Function (ACF) obtained after pilots equalization

The weights $w[n]$ of the RPR filter can be obtained by solving a system of linear equations:

$$R_{out}[l] = \sum_{n=-L}^{L} w[n] R_{eq}[l-n] = \begin{cases} 1 & l = 0 \\ 0 & |l| \leq L, l \neq 0 \end{cases}$$

L is the number of time bins included in the desired side peaks free area (L>6000 for the considered surveillance area)

To reduce the computational load,
- the equations can be properly resampled based on the knowledge of the side-peaks positions
- the system can be solved at FFT speed under proper approximations.

Results against the 2k-Mode DVB-T signals

$R_{eq}[l]$

$R_{out}[l]$

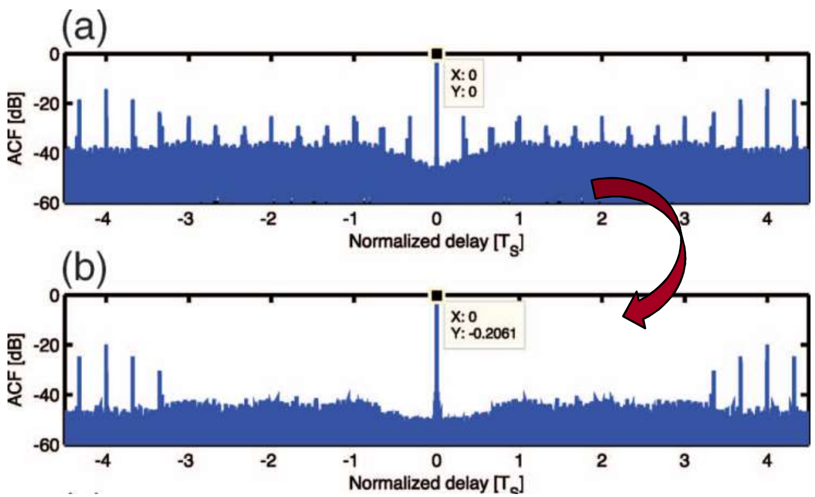

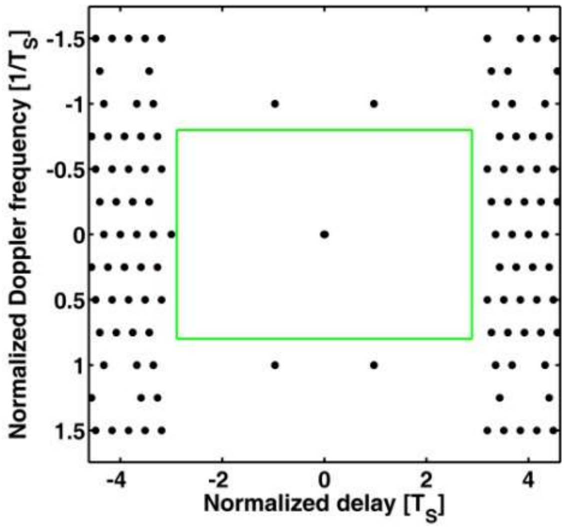

DVB-T Signal Ambiguity Function Control

Results against the 8k-Mode DVB-T signals

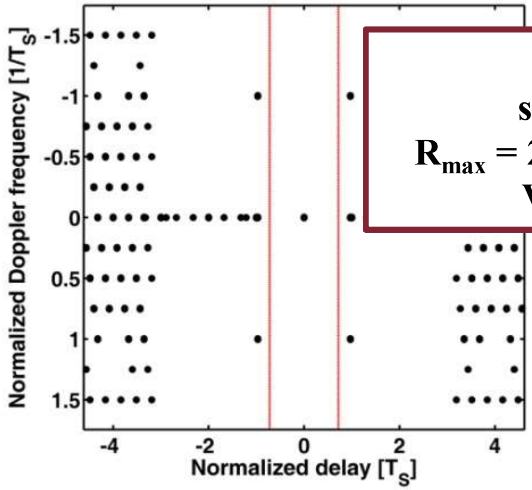

Side-peaks free surveillance area
R_{max} = 200 km ≈ c · 0.75 TSYM
V_{max} = ± 600 m/s

If the maximum bistatic range is limited to $R_{max}=cT_U/3$=89.6 km, the observation region after pilots equalization does not include residual side peaks (no need for RPR)

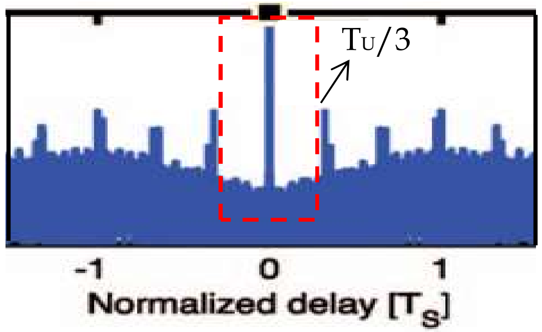

A single subtraction is performed!

<u>Results against real registrations</u>

Original AF

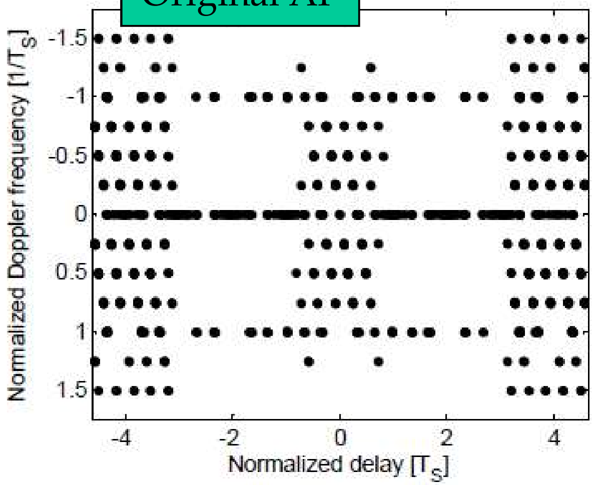

After our approach

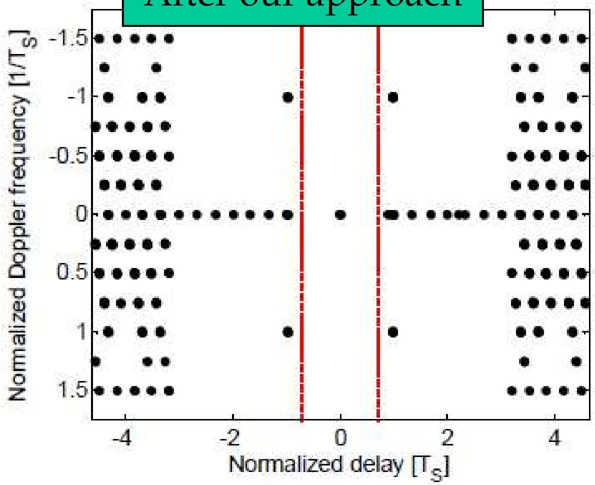

The PBR Receiver

Signal conditioning and ADC + DDC

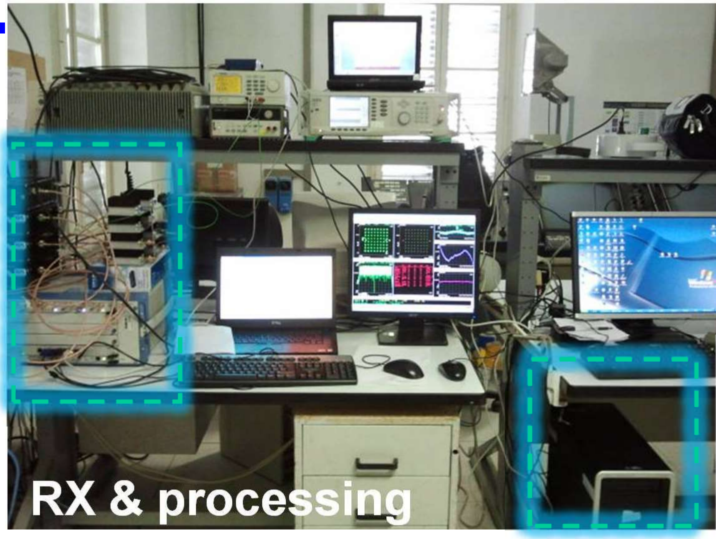

Processing chain

PBR system:

- reference and surveillance Yagi-Uda antennas (UHF) with a gain of 15 dB;
- different signal conditioning for each channel to optimize the input dynamic;
- 12-bit wideband digital receiver/digitizer;
- Sampling frequency of 1.6 GHz;
- FPGAs for real-time digital downconversion (DDC) ;
- locked receiver by GPS signal for the acquisition of DVB-T signal;
- PC for off-line data processing;

The tests in Livorno: Test #1

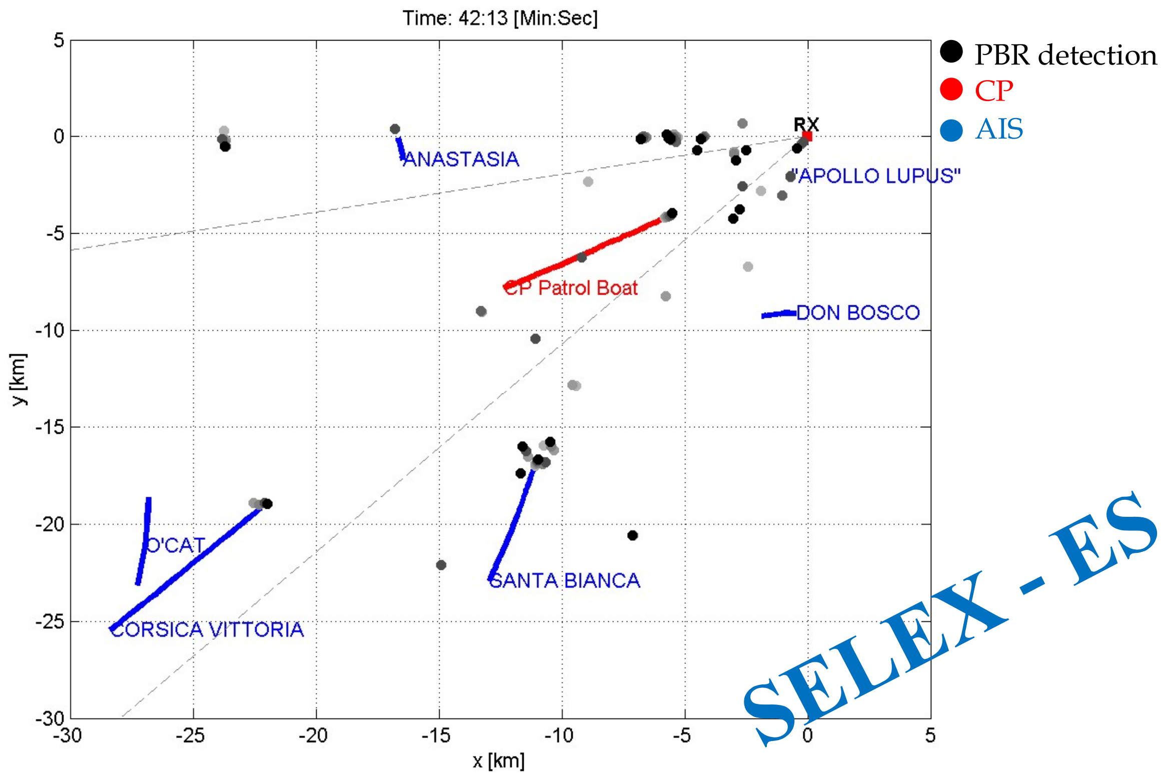

- Estimated detection rate (raw detection for $P_{fa}=10^{-4}$, 3-out-of-3 criterion over the surv. channels): for cooperative target (Coast Guard Patrol boat "Classe 2000"): 71/100
- Again, better performance can be expected using longer CPI (> 1 sec)

The tests in Livorno: Test #2

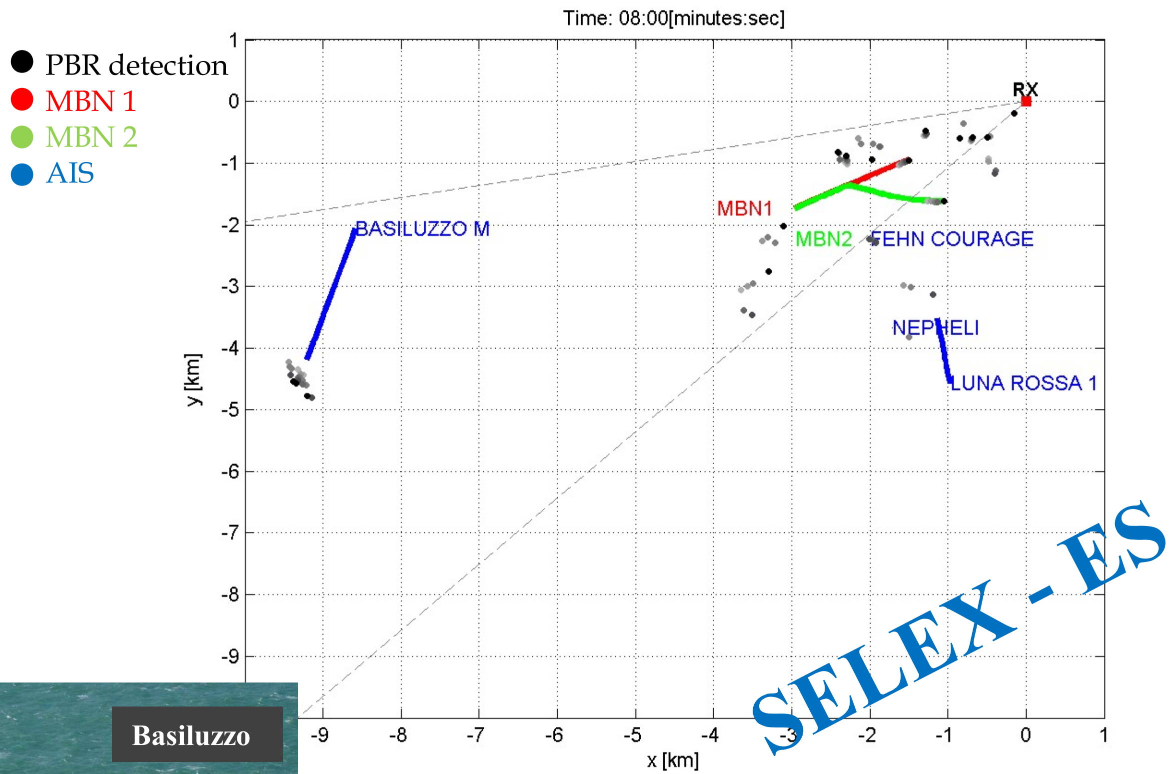

- Estimated detection rate (raw detection for $P_{fa}=10^{-4}$, 3-out-of-3 criterion over the surv. channels) for cooperative targets: 52/62 for MBN1 and 48/62 for MBN2

The tests in Livorno: long range application

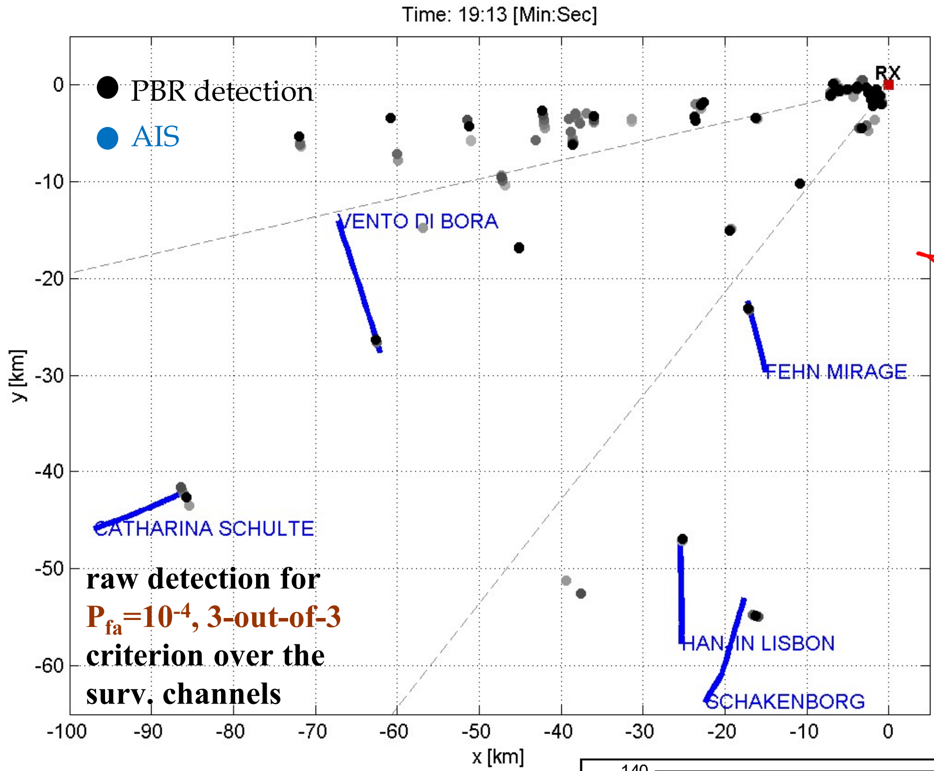

Name	Raw Det.
Catharina Schulte	73/132
Hanjin	72/132
Schackerborg	72/132
Vento di Bora	33/132

Tx altitude 860 m

a looser constraint on the expected radar horizon.

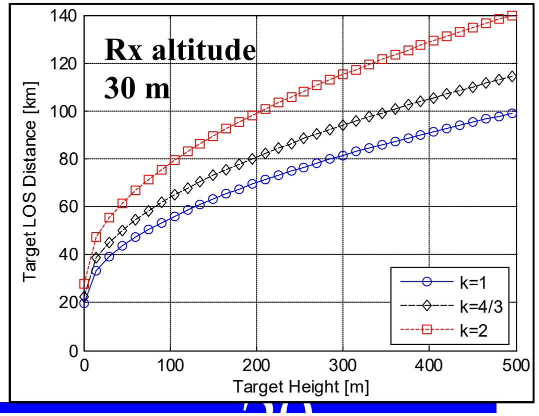

Small Air Vehicles Traffic: WiFi based PR (I)

TEST A

A small aircraft moved on the runway just after landing

- ❑ The small aircraft is continuously detected along its trajectory
- ❑ A good agreement is observed between PBR results and available ground-truth

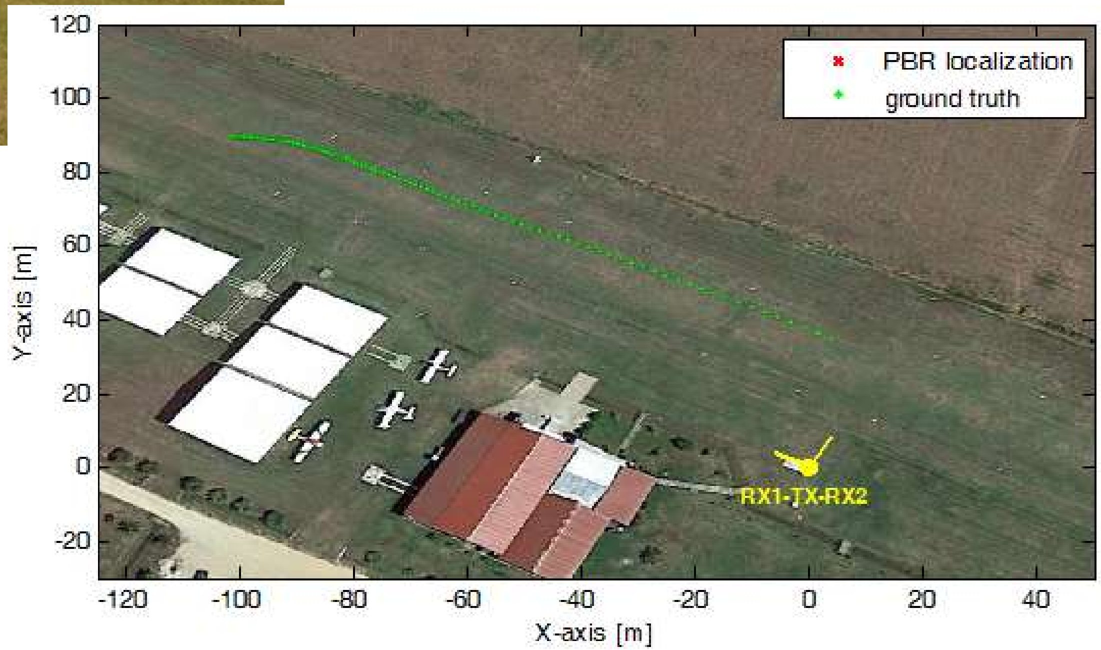

Small Air Vehicles Traffic: WiFi based PR (II)

TEST C

A powered paraglider is flying over the runway involved in a 'touch and go' maneuver.

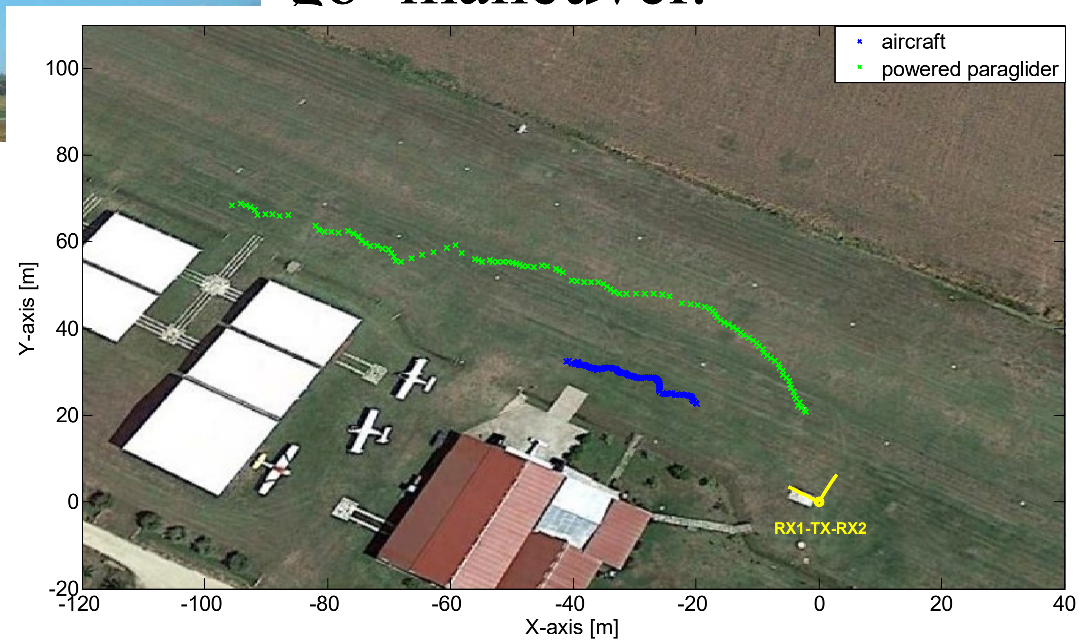

The two sequences of plots clearly reveal the presence of the observed targets

Small Air Vehicles Traffic: WiFi based PR (III)

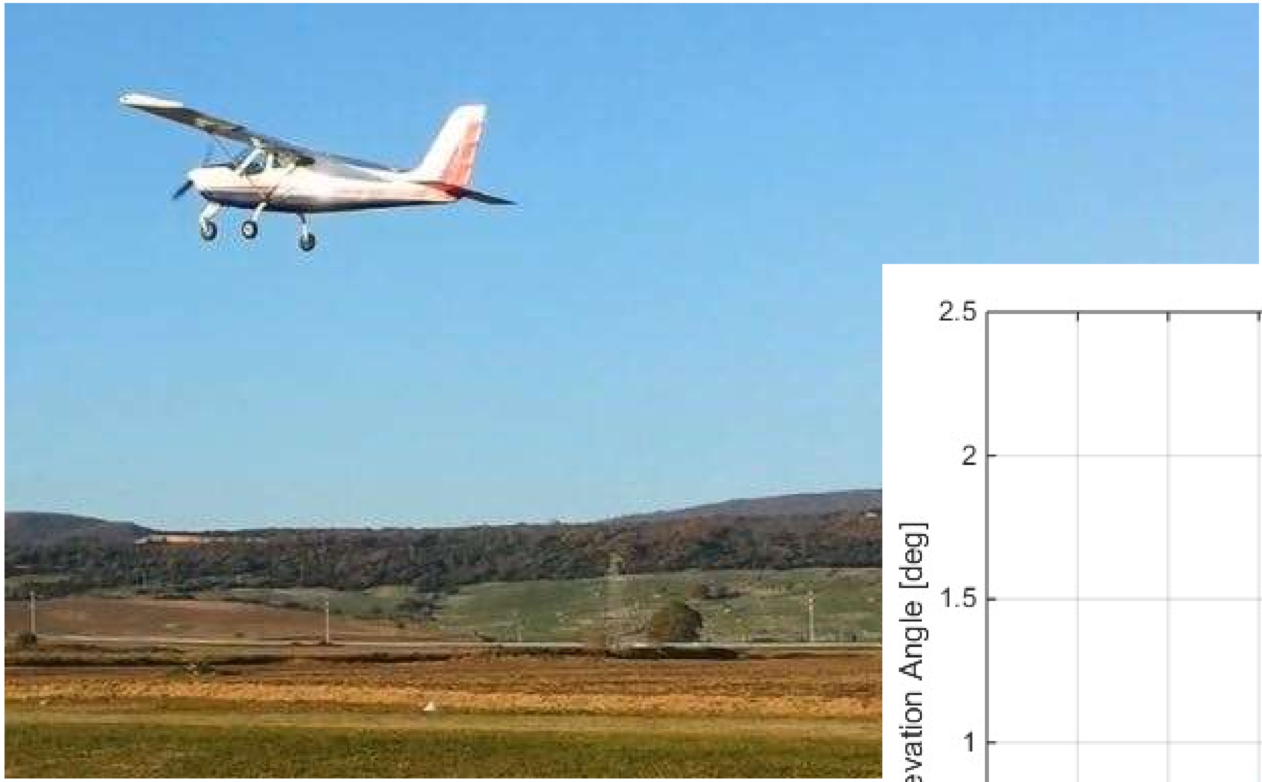

Elevation estimation.

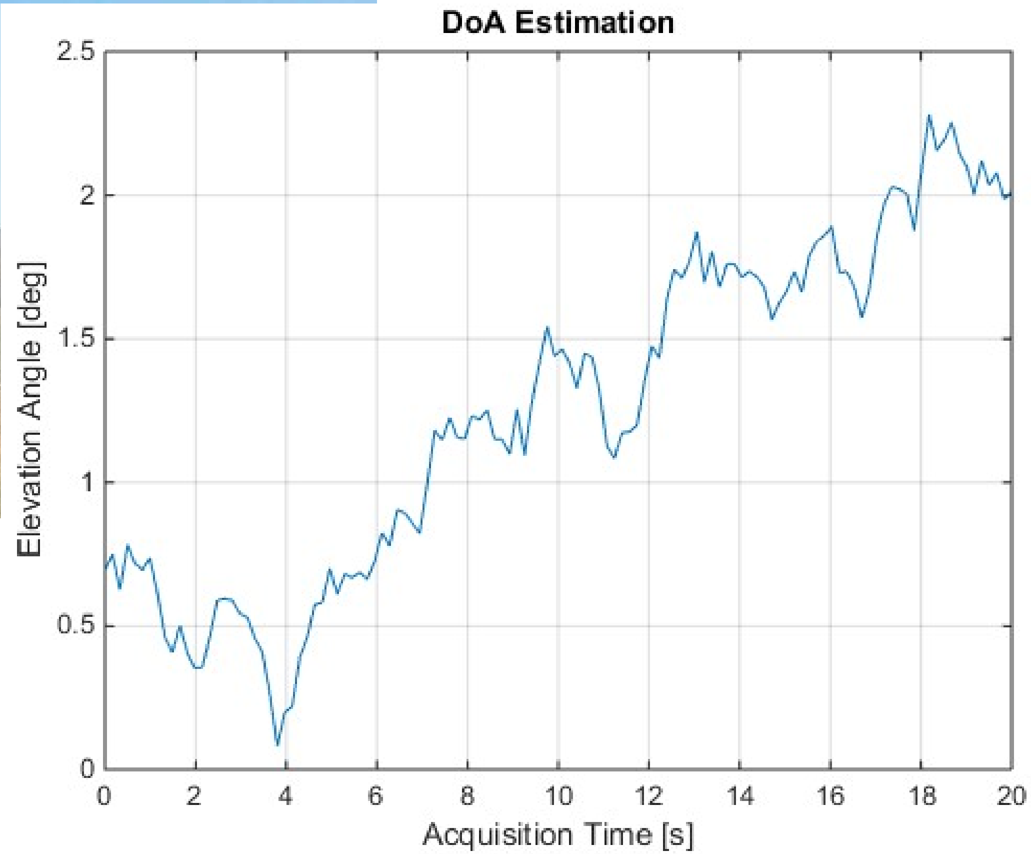

Small UAVs Traffic: WiFi based PR (I)

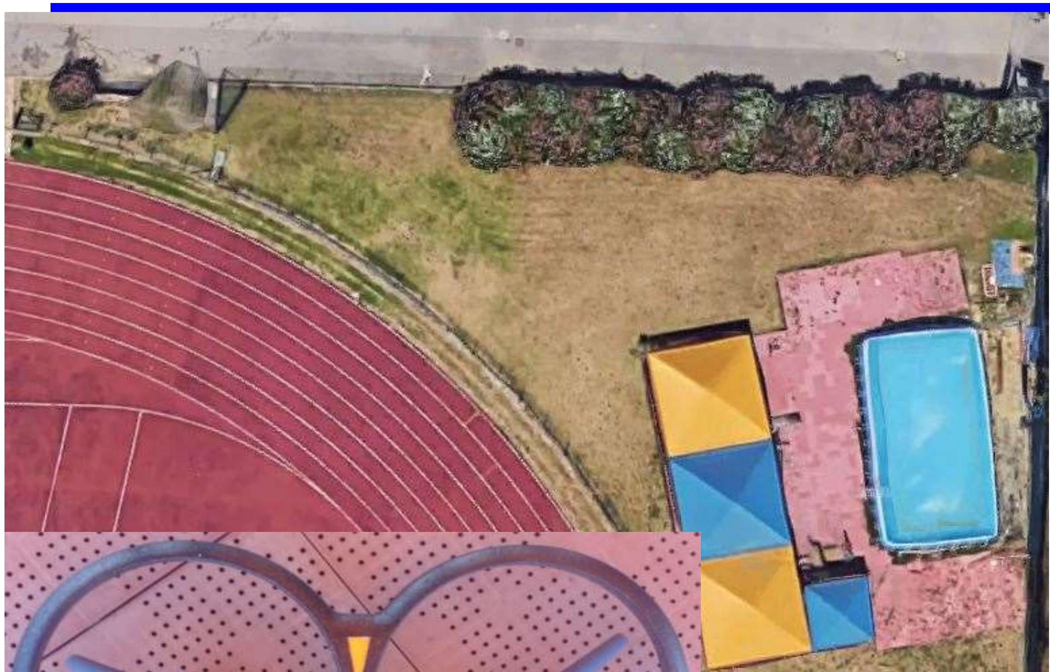

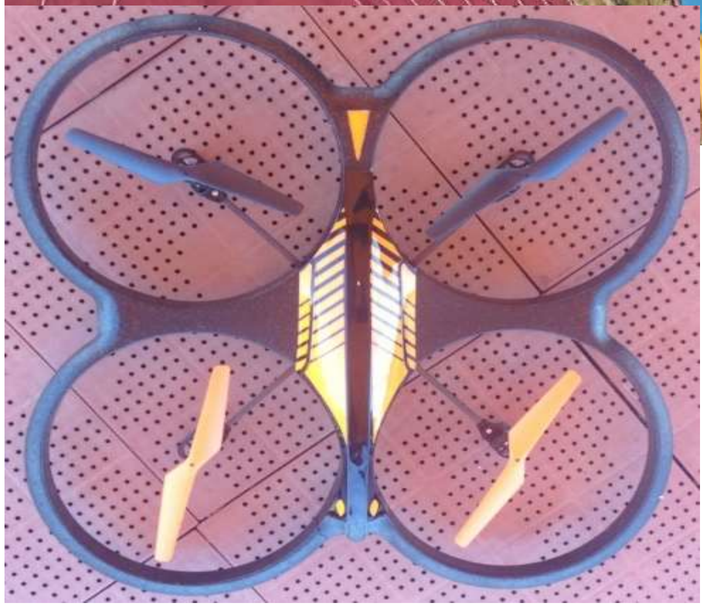

Size: 60 cm x 60 cm x 9 cm
Material:
carbon fiber &
expanded foam

Small UAVs Traffic: WiFi based PR (II)

Dimensions:
60 cm x 60 cm x 9 cm
Material: carbon fiber & expanded foam

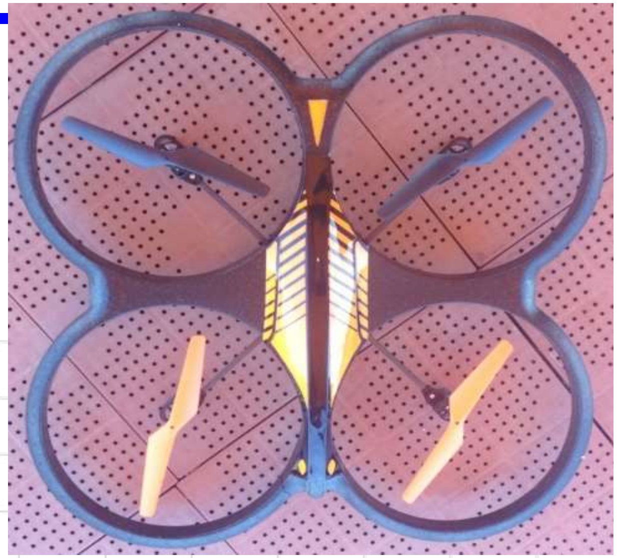

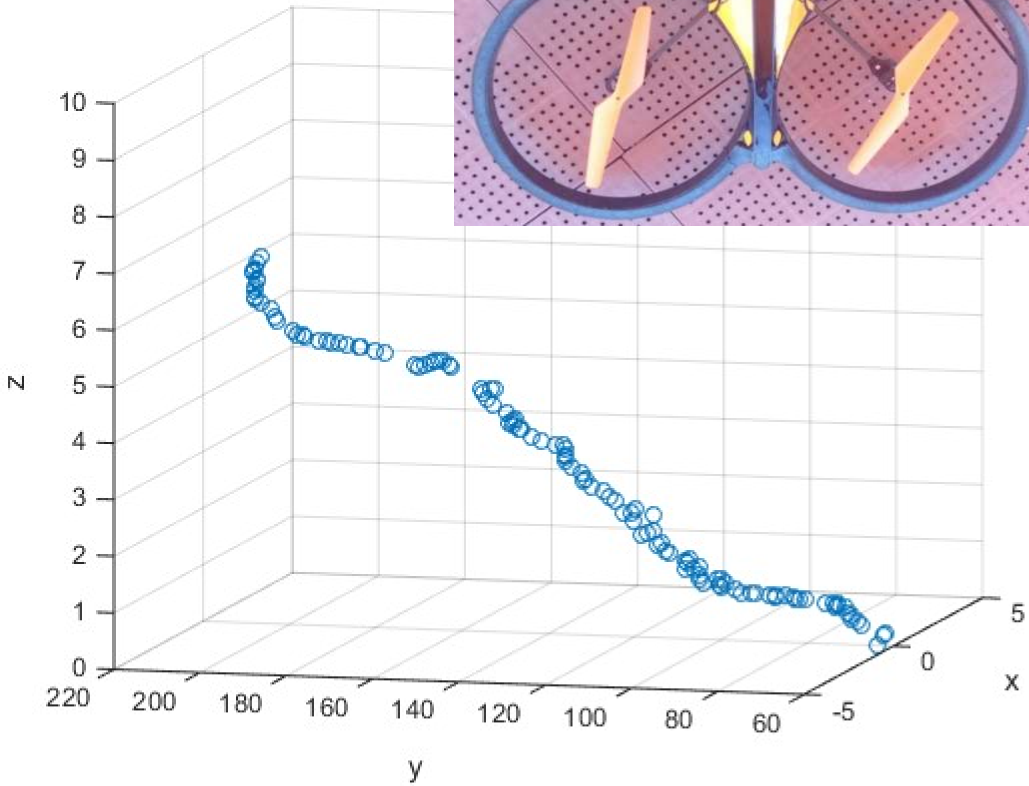

Forward Scatter Radar

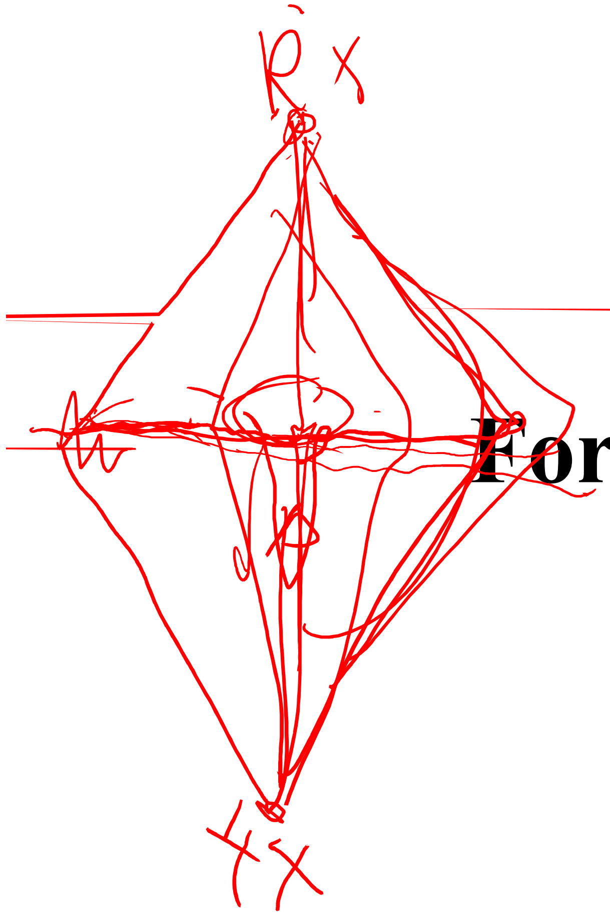

Monostatic vs Forward PBR

Direct Signal Interference: - Monostatic → in different range resolution cells
- Forward → in the same resolution cell

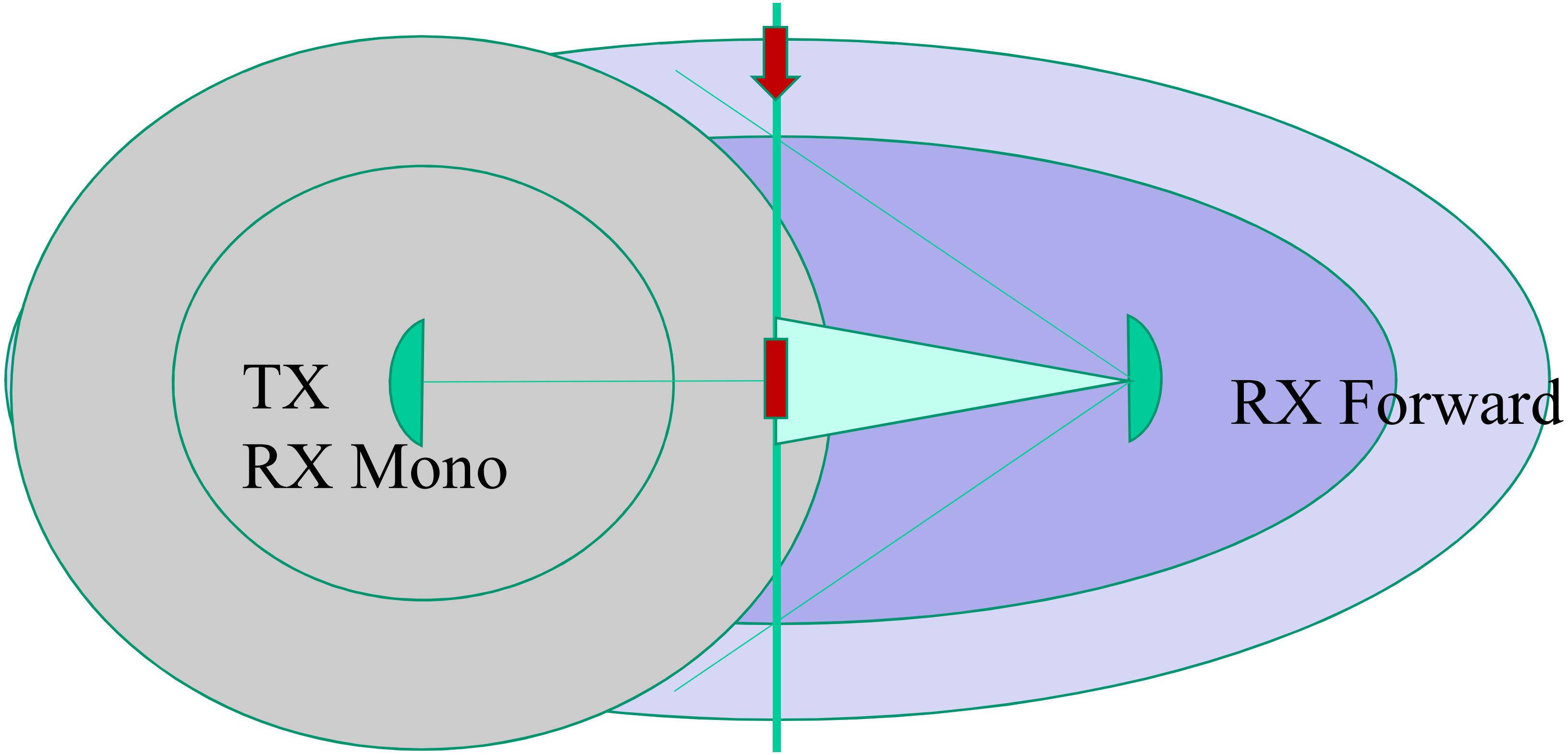

WiFi Experimental Setup

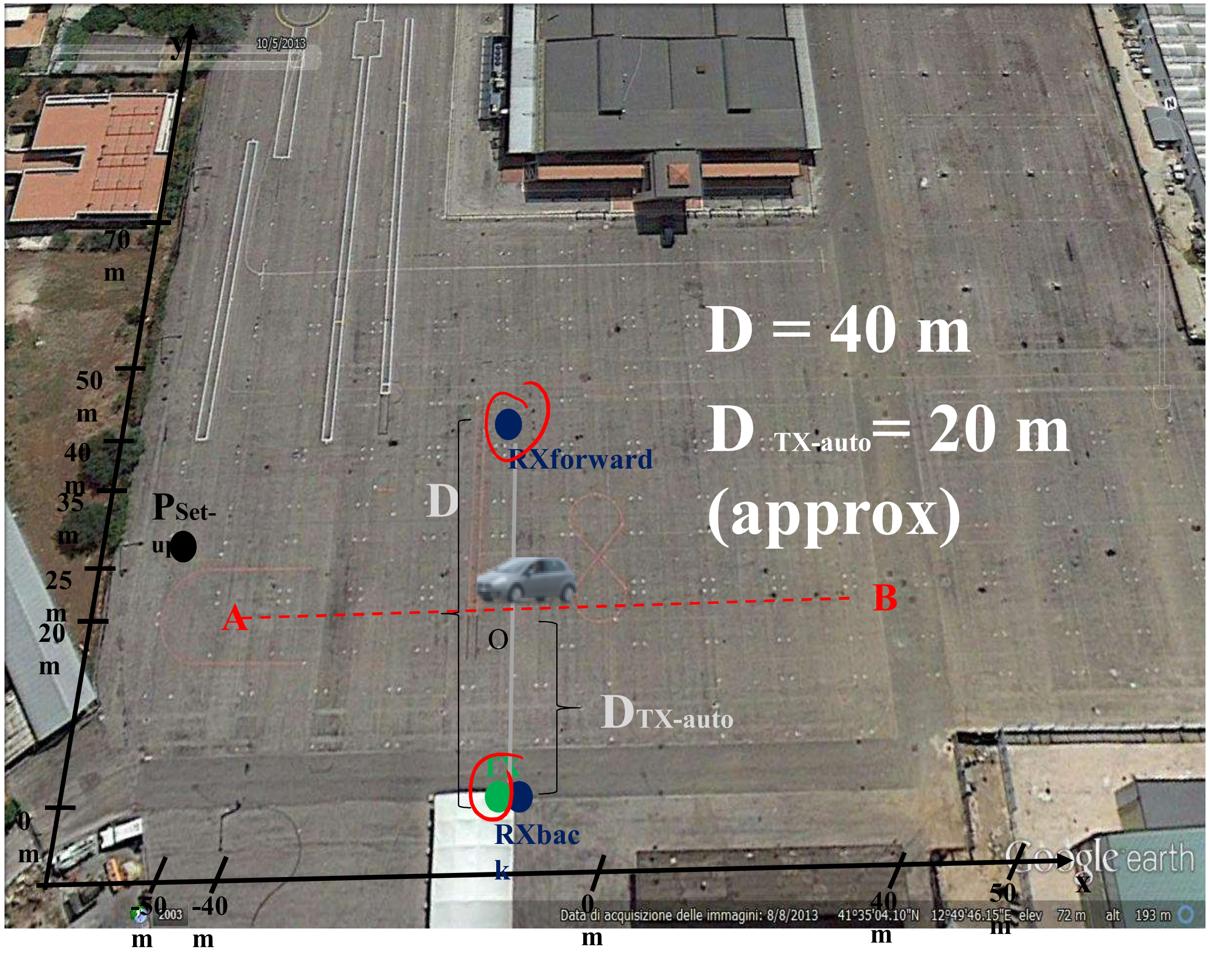

Used vehicles:

- FIAT Punto
- Citroen C3
- Peugeot 107
- VW Polo

Direction:

B --> A

STP – Forward case (tgt2)

STP: Two subsequent acquisitions of the same target

VW
Polo

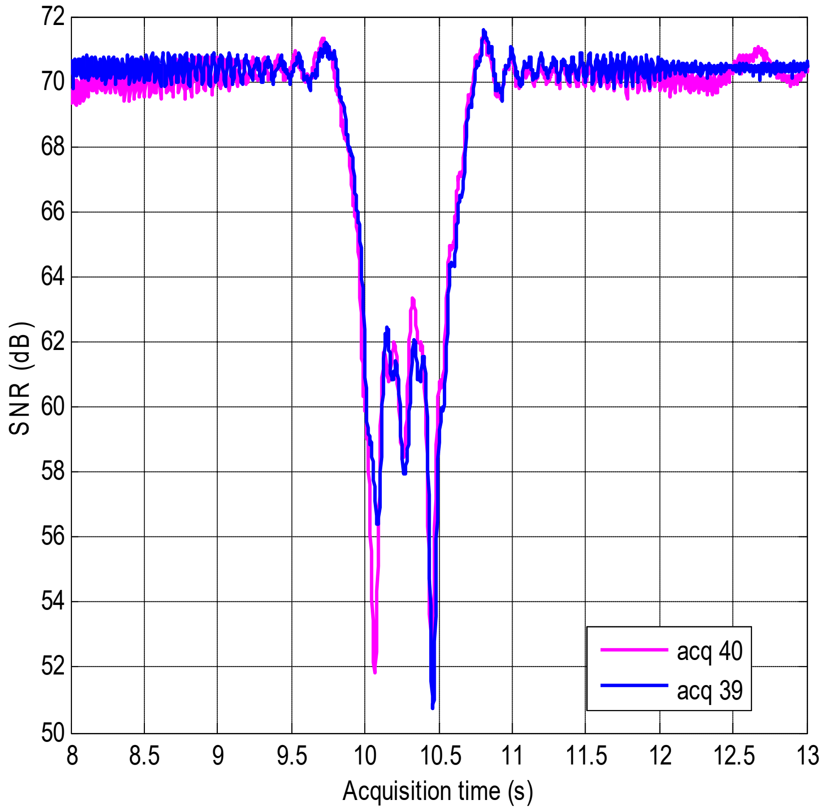

STP – Forward case (tgt1)

STP: Two subsequent acquisitions of the same targets

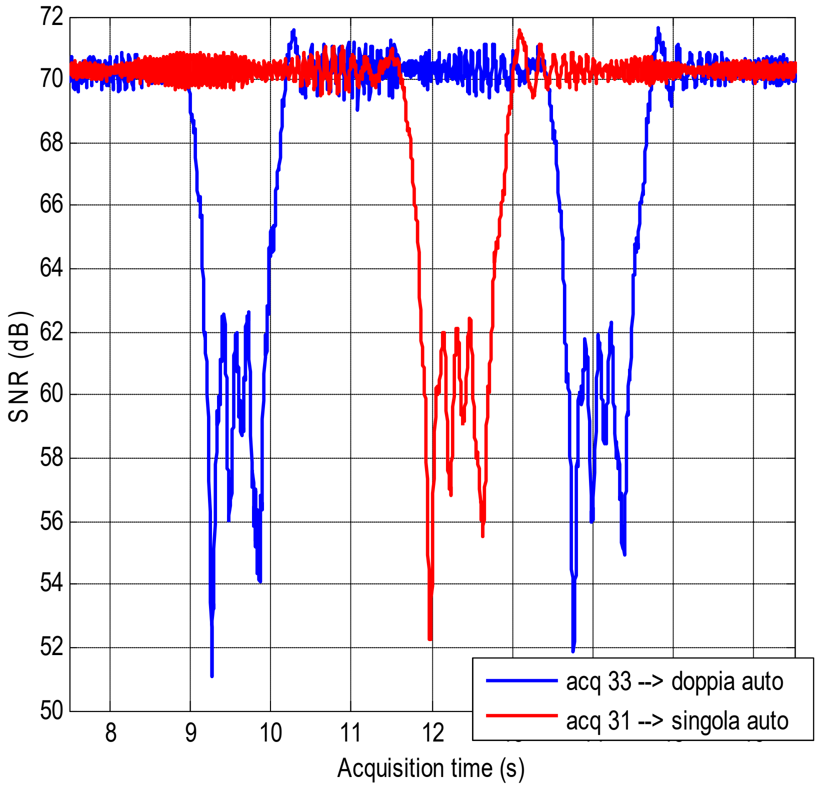

FIAT Punto

High stability both inside the single acquisition and between different acquisitions

STP – Forward case (tgts)

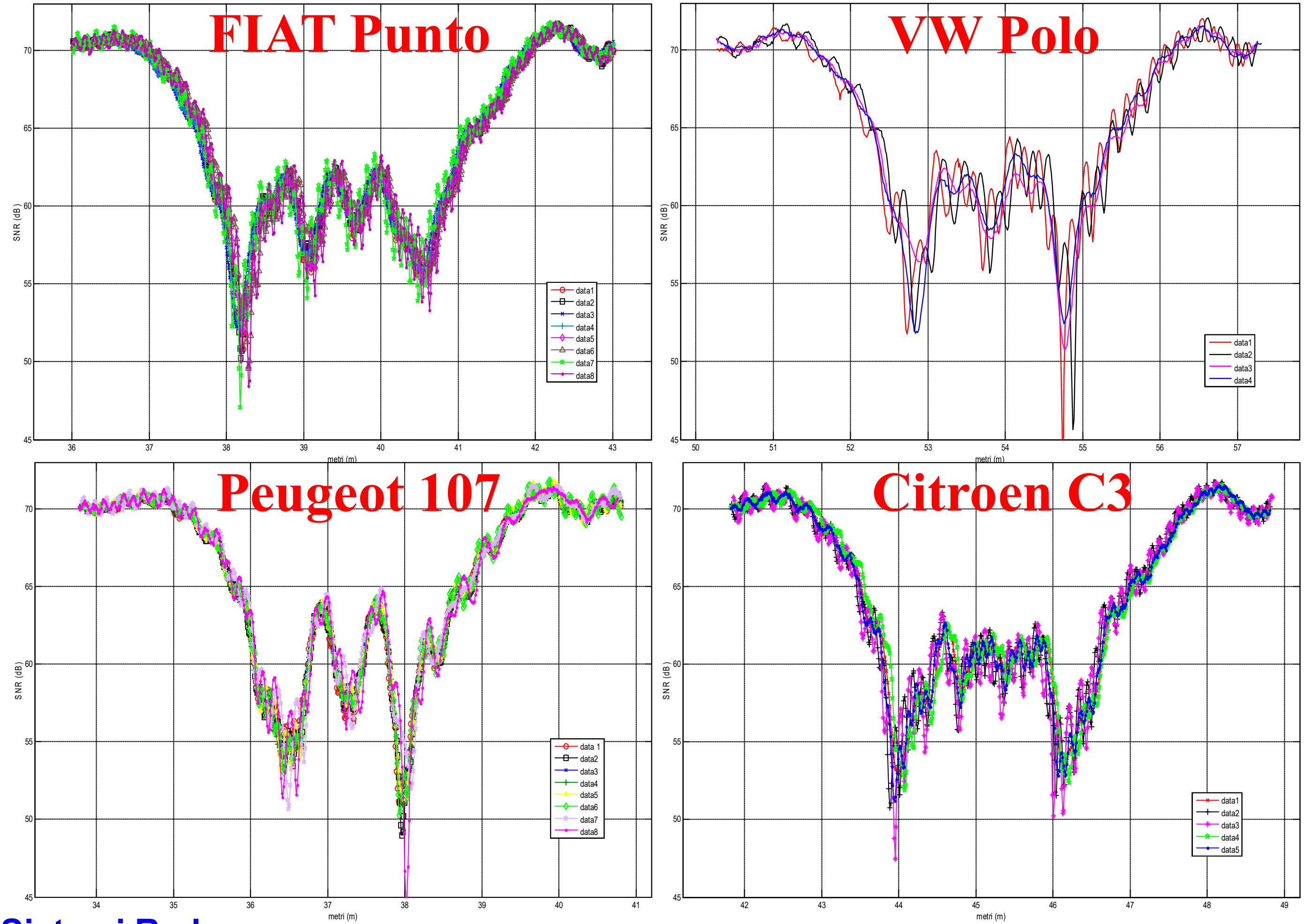

High stability

ML Target Classification

- Classification among hypotheses with same noise variance:

- Hp A: mean vector $\mathbf{x}_A$
- Hp B: mean vector $\mathbf{x}_B$
- Hp C: mean vector $\mathbf{x}_C$
- Hp D: mean vector $\mathbf{x}_D$

- **Likelihood function** $p(\mathbf{x}/H_p A) = \frac{1}{\pi^N \sigma_n^{2N}} e^{-\frac{1}{\sigma_n^{2N}}\left|\mathbf{x}-\mathbf{x}_A\right|^2}$

- **Scaled Logarithmic likelihood :** ***quadratic distance*** $-\left|\mathbf{x}-\mathbf{x}_A\right|^2$

- **ML Classifier:** **Minimum distance**

Target Separability

Distance from		Peugeot 107								FIAT Punto						WV Polo				Citroen C3				
		#1	#2	#3	#4	#5	#6	#7	#8	#9	#10	#11	#12	#13	#14	#15	#16	#17	#18	#19	#20	#21	#22	#23
Peugeot 107	#1	0,0E+0	3,6E+3	3,4E+3	4,1E+3	6,4E+3	8,4E+3	1,8E+4	1,8E+4	3,0E+5	3,2E+5	3,1E+5	3,2E+5	2,8E+5	2,9E+5	1,3E+5	1,4E+5	1,1E+5	9,2E+4	2,5E+5	2,6E+5	2,6E+5	2,3E+5	2,6E+5
	#2	3,6E+3	0,0E+0	2,8E+3	2,6E+3	5,1E+3	9,8E+3	1,9E+4	1,7E+4	3,0E+5	3,1E+5	3,1E+5	3,1E+5	2,7E+5	2,9E+5	1,3E+5	1,3E+5	1,1E+5	9,1E+4	2,4E+5	2,5E+5	2,5E+5	2,3E+5	2,6E+5
	#3	3,4E+3	2,8E+3	0,0E+0	1,5E+3	4,0E+3	7,7E+3	1,6E+4	1,6E+4	3,1E+5	3,3E+5	3,2E+5	3,2E+5	2,8E+5	3,0E+5	1,3E+5	1,4E+5	1,1E+5	9,1E+4	2,5E+5	2,6E+5	2,7E+5	2,4E+5	2,7E+5
	#4	4,1E+3	2,6E+3	1,5E+3	0,0E+0	4,8E+3	9,8E+3	2,0E+4	1,7E+4	2,9E+5	3,1E+5	3,0E+5	3,0E+5	2,7E+5	2,8E+5	1,2E+5	1,3E+5	1,0E+5	8,4E+4	2,3E+5	2,4E+5	2,5E+5	2,2E+5	2,5E+5
	#5	6,4E+3	5,1E+3	4,0E+3	4,8E+3	0,0E+0	1,1E+4	1,9E+4	1,9E+4	3,1E+5	3,3E+5	3,2E+5	3,3E+5	2,9E+5	3,1E+5	1,4E+5	1,4E+5	1,2E+5	9,8E+4	2,6E+5	2,7E+5	2,7E+5	2,4E+5	2,7E+5
	#6	8,4E+3	9,8E+3	7,7E+3	9,7E+3	1,1E+4	0,0E+0	2,1E+4	2,3E+4	3,4E+5	3,6E+5	3,5E+5	3,6E+5	3,1E+5	3,3E+5	1,5E+5	1,5E+5	1,3E+5	1,1E+5	2,8E+5	2,9E+5	3,0E+5	2,6E+5	3,0E+5
	#7	1,8E+4	1,9E+4	1,6E+4	2,0E+4	1,9E+4	2,1E+4	0,0E+0	3,2E+4	3,5E+5	3,6E+5	3,6E+5	3,6E+5	3,2E+5	3,4E+5	1,5E+5	1,5E+5	1,3E+5	1,1E+5	2,9E+5	3,0E+5	3,0E+5	2,7E+5	3,1E+5
	#8	1,8E+4	1,8E+4	1,6E+4	1,7E+4	1,9E+4	2,3E+4	3,2E+4	0,0E+0	3,3E+5	3,4E+5	3,5E+5	3,5E+5	3,1E+5	3,2E+5	1,4E+5	1,3E+5	1,2E+5	1,1E+5	2,7E+5	2,8E+5	2,9E+5	2,5E+5	2,9E+5
FIAT Punto	#9	3,0E+5	3,0E+5	3,1E+5	2,9E+5	3,2E+5	3,4E+5	3,5E+5	3,3E+5	0,0E+0	3,4E+3	2,3E+3	2,8E+3	1,6E+4	1,5E+4	1,6E+5	2,1E+5	1,5E+5	1,4E+5	2,3E+4	3,4E+4	3,9E+4	2,7E+4	2,5E+4
	#10	3,2E+5	3,1E+5	3,3E+5	3,1E+5	3,4E+5	3,6E+5	3,6E+5	3,4E+5	3,4E+3	0,0E+0	2,0E+3	2,1E+3	1,8E+4	1,6E+4	1,6E+5	2,0E+5	1,5E+5	1,5E+5	2,3E+4	3,4E+4	4,0E+4	2,8E+4	2,6E+4
	#11	3,1E+5	3,1E+5	3,2E+5	3,0E+5	3,3E+5	3,5E+5	3,6E+5	3,5E+5	2,3E+3	2,0E+3	0,0E+0	4,2E+2	1,7E+4	1,5E+4	1,7E+5	2,4E+5	1,8E+5	1,6E+5	2,2E+4	3,4E+4	4,1E+4	3,0E+4	2,6E+4
	#12	3,2E+5	3,1E+5	3,3E+5	3,1E+5	3,3E+5	3,6E+5	3,7E+5	3,5E+5	2,8E+3	2,1E+3	4,2E+2	0,0E+0	1,8E+4	1,5E+4	1,7E+5	2,3E+5	1,7E+5	1,6E+5	2,4E+4	3,5E+4	4,2E+4	2,9E+4	2,7E+4
	#13	2,8E+5	2,7E+5	2,9E+5	2,7E+5	2,9E+5	3,1E+5	3,2E+5	3,1E+5	1,7E+4	1,8E+4	1,7E+4	1,8E+4	0,0E+0	1,6E+4	1,5E+5	2,0E+5	1,5E+5	1,3E+5	3,2E+4	4,3E+4	5,0E+4	3,4E+4	3,6E+4
	#14	2,9E+5	2,9E+5	3,0E+5	2,8E+5	3,1E+5	3,3E+5	3,4E+5	3,1E+5	1,5E+4	1,6E+4	1,4E+4	1,5E+4	1,6E+4	0,0E+0	1,5E+5	1,6E+5	1,2E+5	1,4E+5	3,2E+4	4,3E+4	5,2E+4	3,5E+4	3,6E+4
WV Polo	#15	1,3E+5	1,3E+5	1,3E+5	1,2E+5	1,4E+5	1,5E+5	1,5E+5	1,4E+5	1,5E+5	1,6E+5	1,7E+5	1,7E+5	1,5E+5	1,5E+5	0,0E+0	3,8E+4	3,6E+4	3,2E+4	1,0E+5	1,3E+5	1,6E+5	1,0E+5	1,2E+5
	#16	1,4E+5	1,3E+5	1,4E+5	1,3E+5	1,4E+5	1,5E+5	1,5E+5	1,3E+5	2,1E+5	2,0E+5	2,4E+5	2,3E+5	2,0E+5	1,7E+5	3,9E+4	0,0E+0	3,3E+4	3,1E+4	1,4E+5	1,9E+5	2,3E+5	1,1E+5	1,7E+5
	#17	1,1E+5	1,1E+5	1,1E+5	1,0E+5	1,2E+5	1,3E+5	1,3E+5	1,2E+5	1,5E+5	1,5E+5	1,8E+5	1,7E+5	1,5E+5	1,2E+5	3,7E+4	3,3E+4	0,0E+0	1,0E+4	8,2E+4	1,3E+5	1,6E+5	6,6E+4	1,1E+5
	#18	9,1E+4	9,1E+4	9,1E+4	8,3E+4	9,8E+4	1,1E+5	1,1E+5	1,1E+5	1,4E+5	1,5E+5	1,5E+5	1,5E+5	1,3E+5	1,3E+5	3,1E+4	3,2E+4	1,0E+4	0,0E+0	8,5E+4	1,1E+5	1,3E+5	8,1E+4	9,9E+4
Citroen C3	#19	2,5E+5	2,4E+5	2,5E+5	2,3E+5	2,6E+5	2,8E+5	2,9E+5	2,7E+5	2,3E+4	2,3E+4	2,2E+4	2,3E+4	3,2E+4	3,2E+4	1,0E+5	1,4E+5	8,3E+4	8,4E+4	0,0E+0	1,5E+4	2,1E+4	3,4E+3	4,1E+3
	#20	2,6E+5	2,5E+5	2,6E+5	2,4E+5	2,7E+5	2,9E+5	3,0E+5	2,7E+5	3,4E+4	3,4E+4	3,4E+4	3,5E+4	4,4E+4	4,3E+4	1,3E+5	1,9E+5	1,3E+5	1,1E+5	1,5E+4	0,0E+0	3,1E+4	1,4E+4	1,1E+4
	#21	2,6E+5	2,5E+5	2,7E+5	2,5E+5	2,7E+5	3,0E+5	3,1E+5	2,9E+5	3,9E+4	4,0E+4	4,1E+4	4,3E+4	5,0E+4	5,1E+4	1,6E+5	2,3E+5	1,6E+5	1,3E+5	2,0E+4	3,1E+4	0,0E+0	2,5E+4	2,1E+4
	#22	2,3E+5	2,3E+5	2,4E+5	2,2E+5	2,4E+5	2,6E+5	2,7E+5	2,5E+5	2,7E+4	2,8E+4	3,0E+4	2,8E+4	3,4E+4	3,5E+4	1,0E+5	1,1E+5	6,6E+4	8,2E+4	3,4E+3	1,4E+4	2,5E+4	0,0E+0	7,8E+3
	#23	2,6E+5	2,6E+5	2,7E+5	2,5E+5	2,7E+5	3,0E+5	3,1E+5	2,8E+5	2,5E+4	2,6E+4	2,6E+4	2,7E+4	3,7E+4	3,6E+4	1,2E+5	1,7E+5	1,1E+5	9,9E+4	4,0E+3	1,1E+4	2,1E+4	7,7E+3	0,0E+0
Peugeot 107	MIN	1,8E+4	1,9E+4	1,6E+4	2,0E+4	1,9E+4	2,3E+4	3,2E+4	3,2E+4	2,9E+5	3,1E+5	3,0E+5	3,0E+5	2,7E+5	2,8E+5	1,2E+5	1,3E+5	1,0E+5	8,4E+4	2,3E+5	2,4E+5	2,5E+5	2,2E+5	2,5E+5
FIAT Punto	MIN	2,8E+5	2,7E+5	2,9E+5	2,7E+5	2,9E+5	3,1E+5	3,2E+5	3,1E+5	1,7E+4	1,8E+4	1,7E+4	1,8E+4	1,8E+4	1,6E+4	1,5E+5	1,6E+5	1,2E+5	1,3E+5	2,2E+4	3,4E+4	3,9E+4	2,7E+4	2,5E+4
WV Polo	MIN	9,1E+4	9,1E+4	9,1E+4	8,3E+4	9,8E+4	1,1E+5	1,1E+5	1,1E+5	1,4E+5	1,5E+5	1,5E+5	1,5E+5	1,3E+5	1,2E+5	3,9E+4	3,8E+4	3,6E+4	3,2E+4	8,2E+4	1,1E+5	1,3E+5	6,6E+4	9,9E+4
Citroen C3	MIN	2,3E+5	2,3E+5	2,4E+5	2,2E+5	2,4E+5	2,6E+5	2,7E+5	2,5E+5	2,3E+4	2,3E+4	2,2E+4	2,3E+4	3,2E+4	3,2E+4	1,0E+5	1,1E+5	6,6E+4	8,2E+4	2,0E+4	3,1E+4	3,1E+4	2,5E+4	2,1E+4

GNSS- based Forward Scatter Radar (I)

- **FSR**

- nonmetallic

- small

- low-detecatble

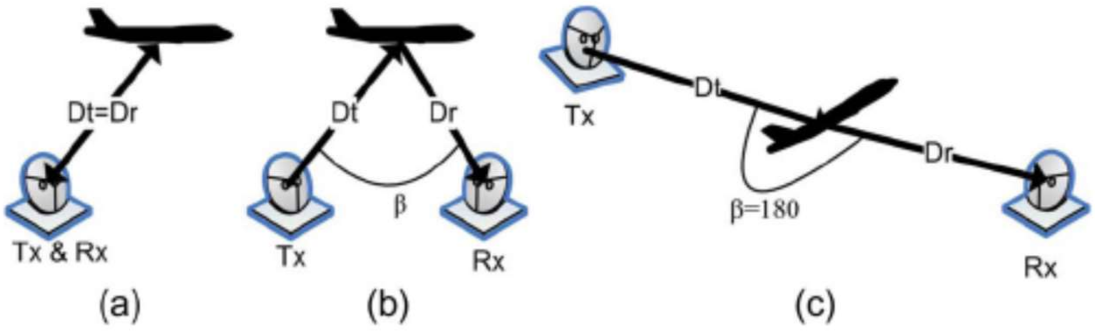

Fig. 1. (a) Monostatic radar. (b) Bistatic radar. (c) FSR.

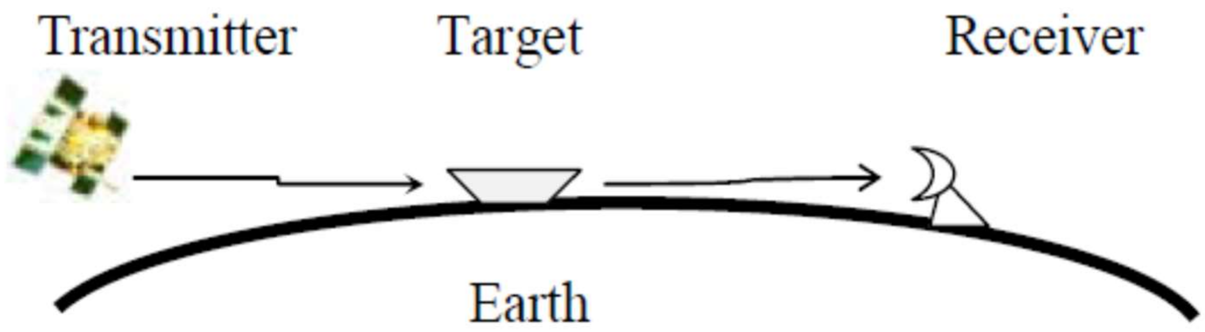

Figure 1. FSR topology

GNSS- based Forward Scatter Radar (II)

- **Crossing Van**

Fig.4. Experimental scenario

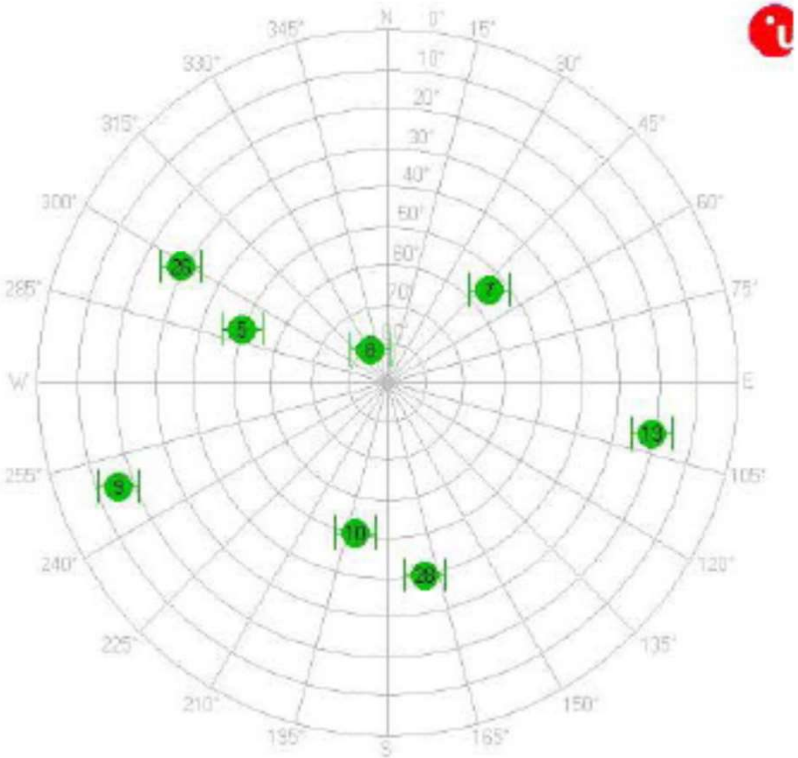

Fig. 5. Satellite constellations

GNSS- based Forward Scatter Radar (III)

Detection of crossing van with satellite 28 signal

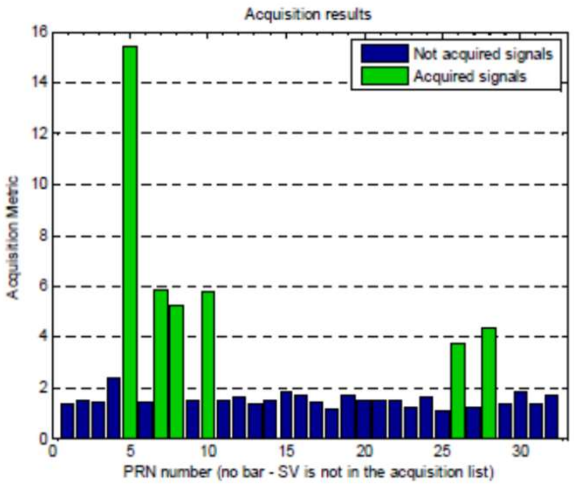

Fig. 6.Acquisition results

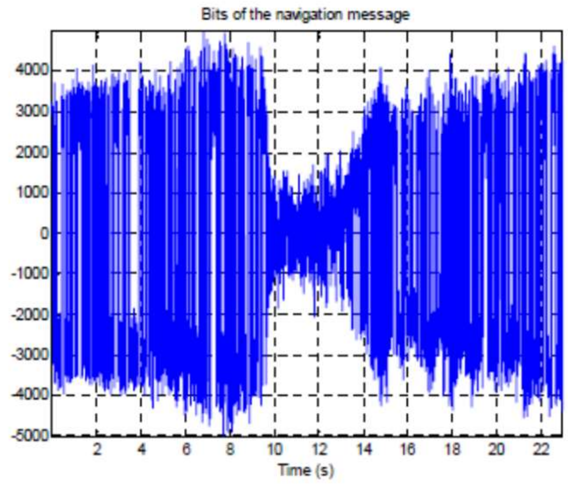

Fig 7. Navigation message of satellite 28

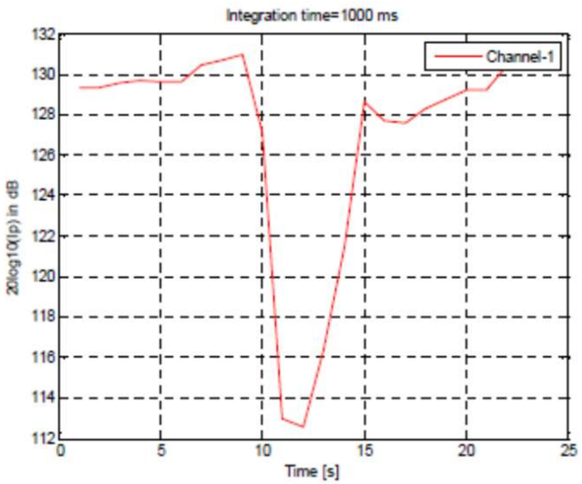

Fig.8. Integrated power (1000ms)

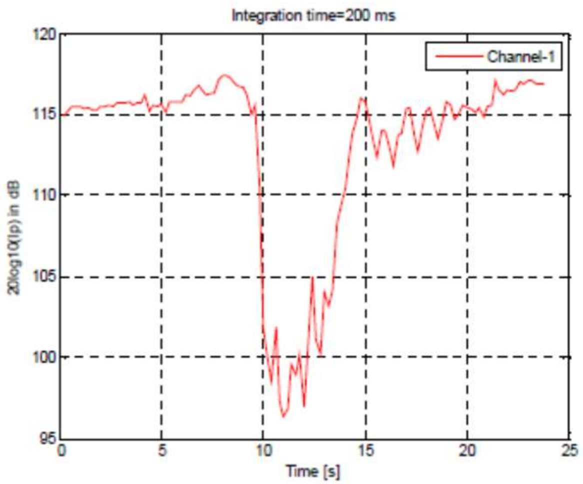

Fig. 9. Integrated power (200ms)

GNSS- based Forward Scatter Radar (IV)

Detection of air traffic

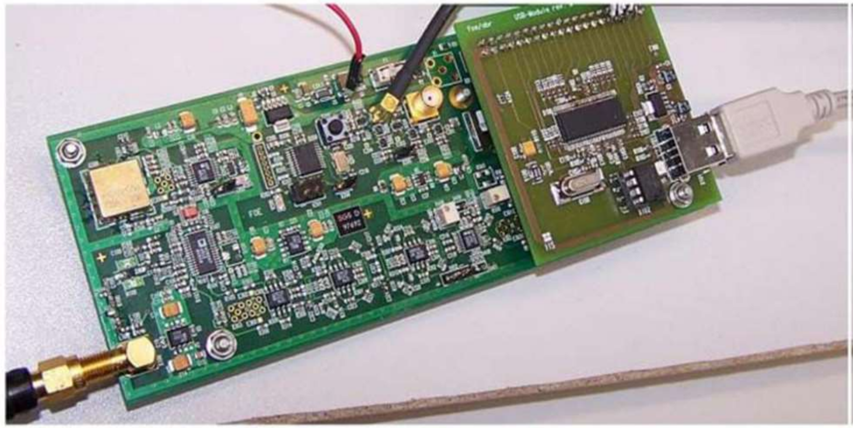

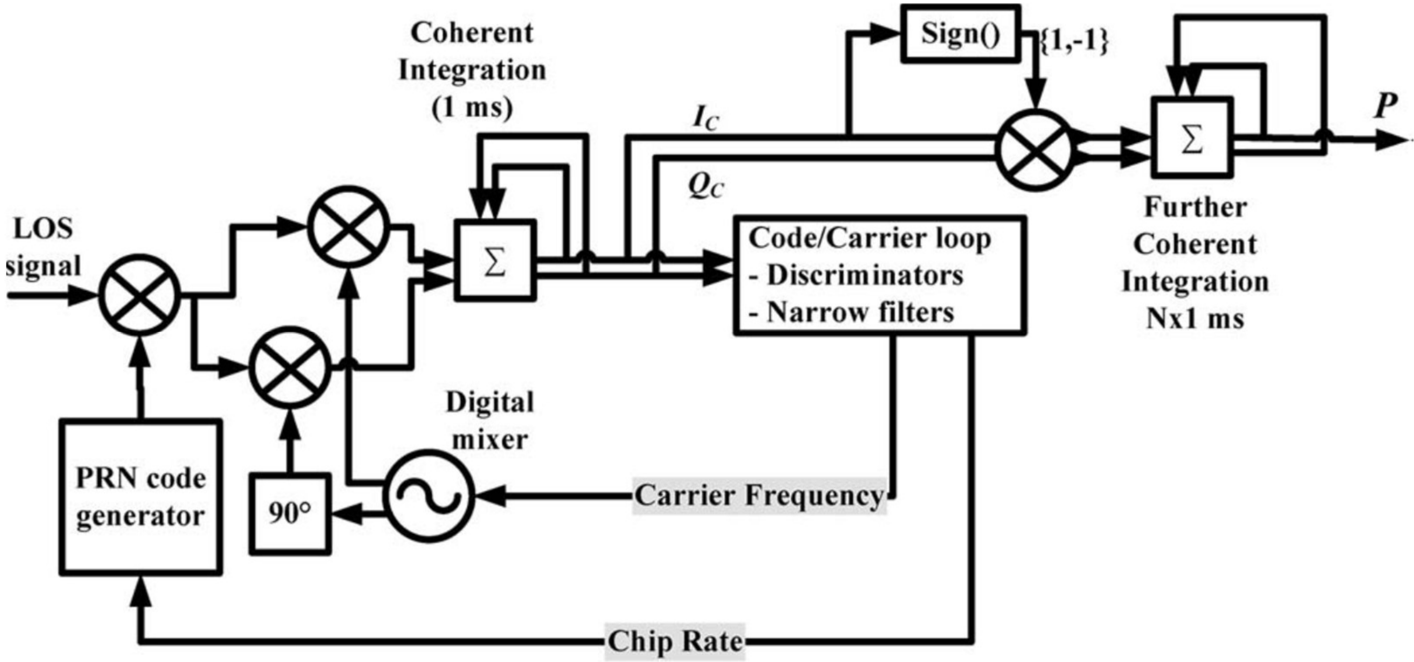

Experimental results - Nuremberg

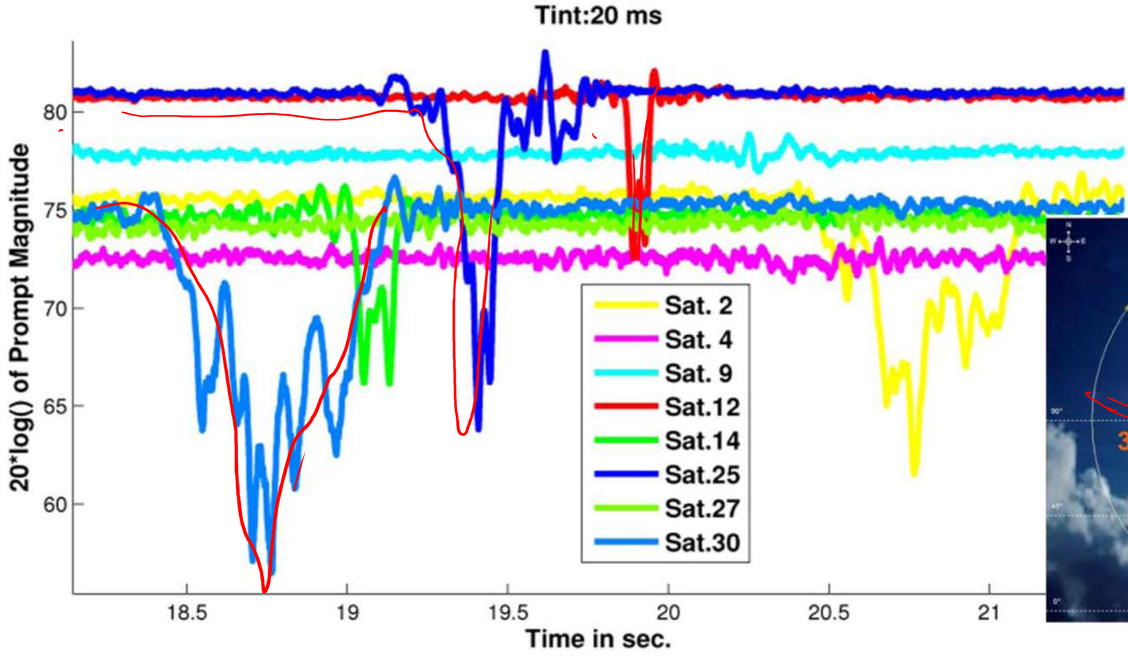

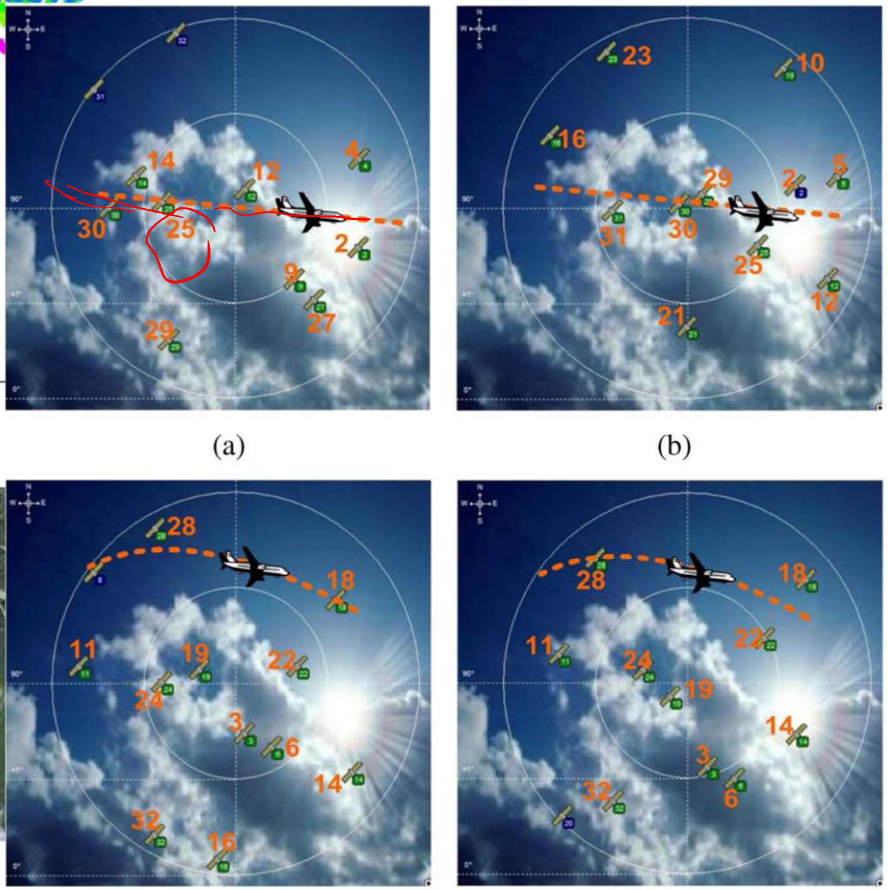

(a) (b) (c) (d)

Forward Scatter Radar : DTV-S (I)

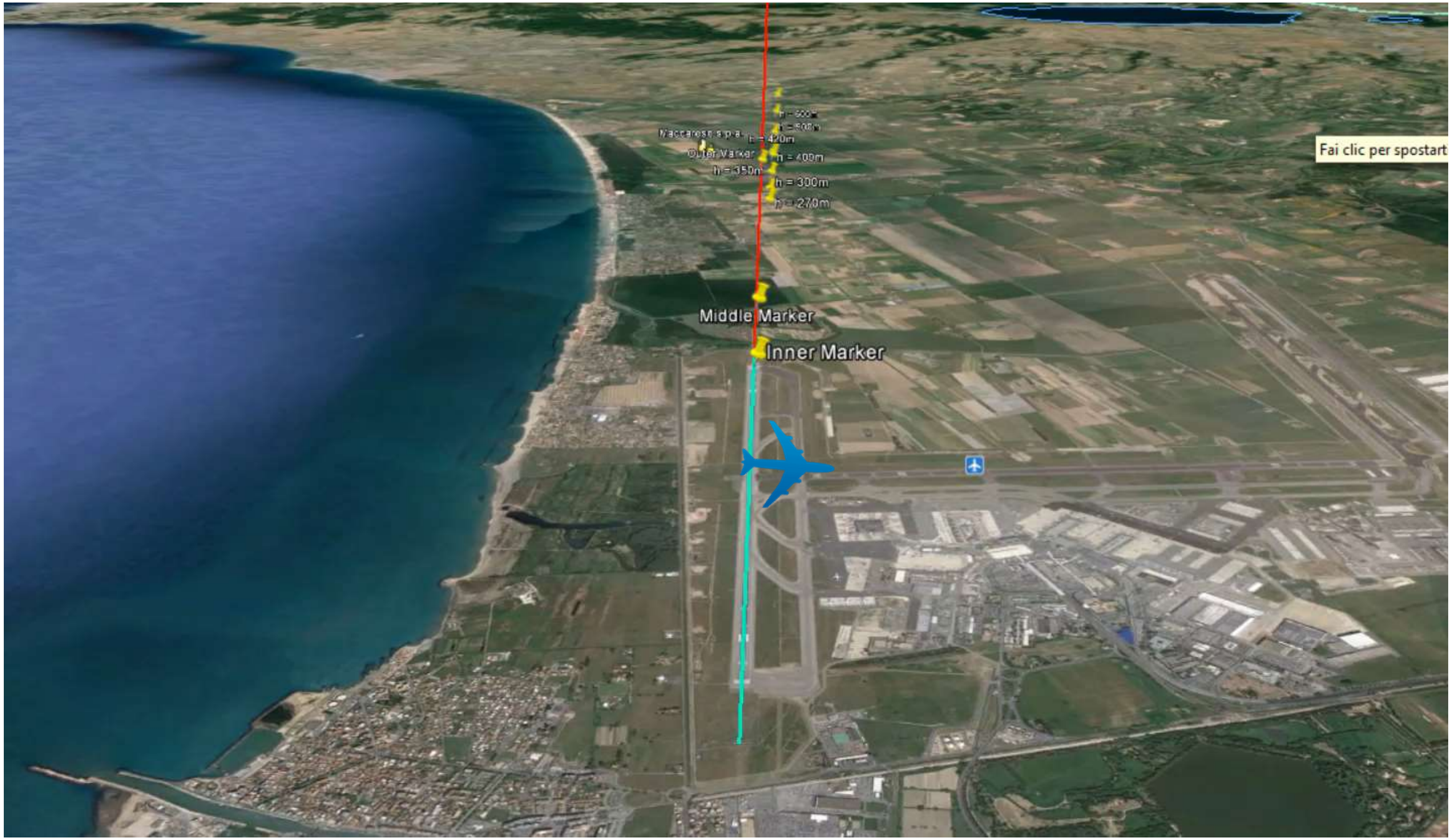

Forward Scatter Radar : DTV-S (II)

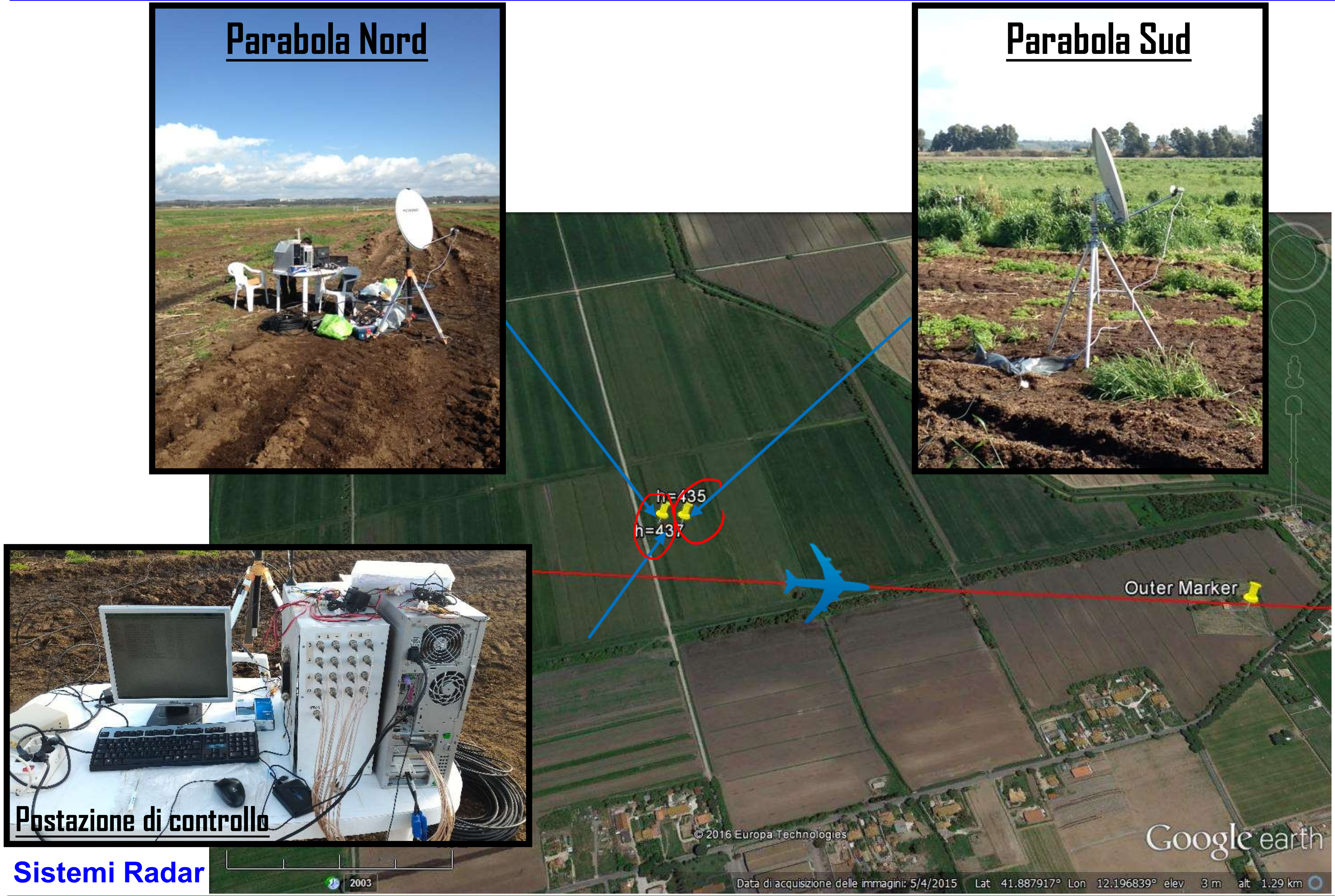

Forward Scatter Radar : DTV-S (III)

❑ Doppler signature extraction

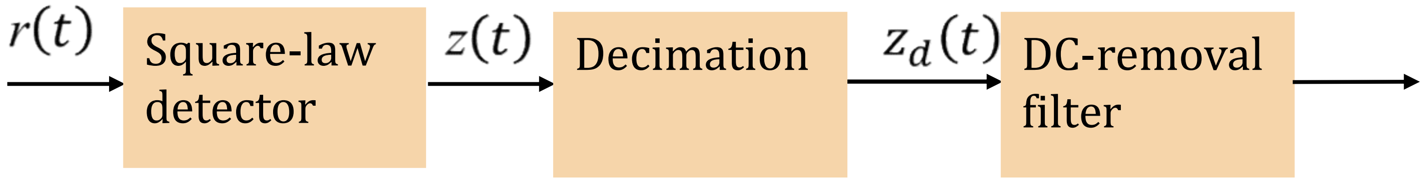

❑ Time domain signatures

❖ *Sampling frequency* $F_s = 25\ MHz$ $F_s = 763\ Hz$

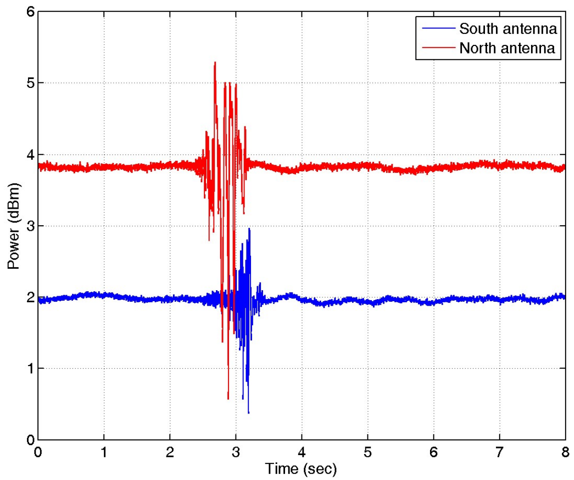

First data set

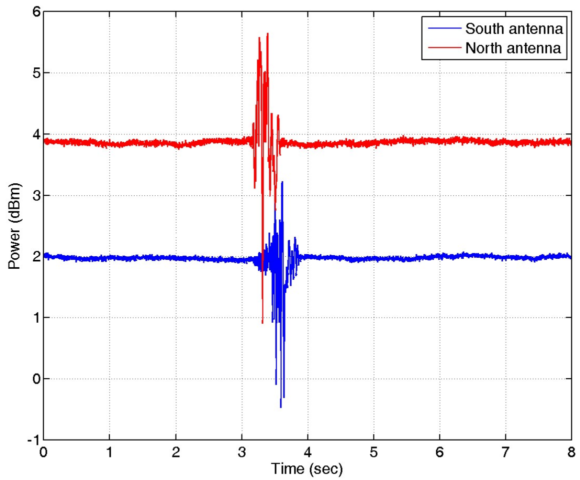

Second data set

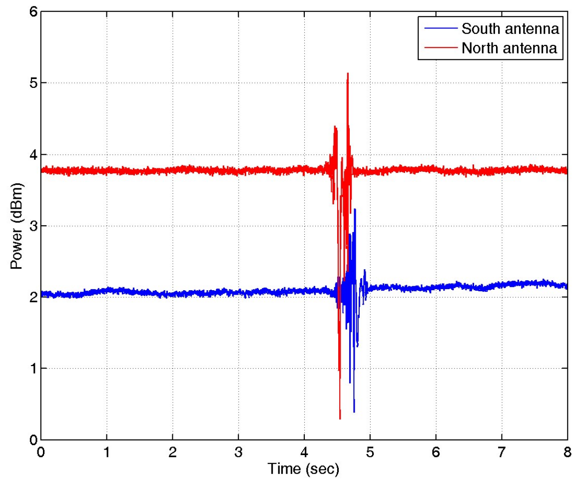

Third data set

✓ The amplitude modulation due to the target crossing the baseline is noticeable.

Forward Scatter Radar : DTV-S (IV)

❖ Single baseline configuration: Spectrogram analysis

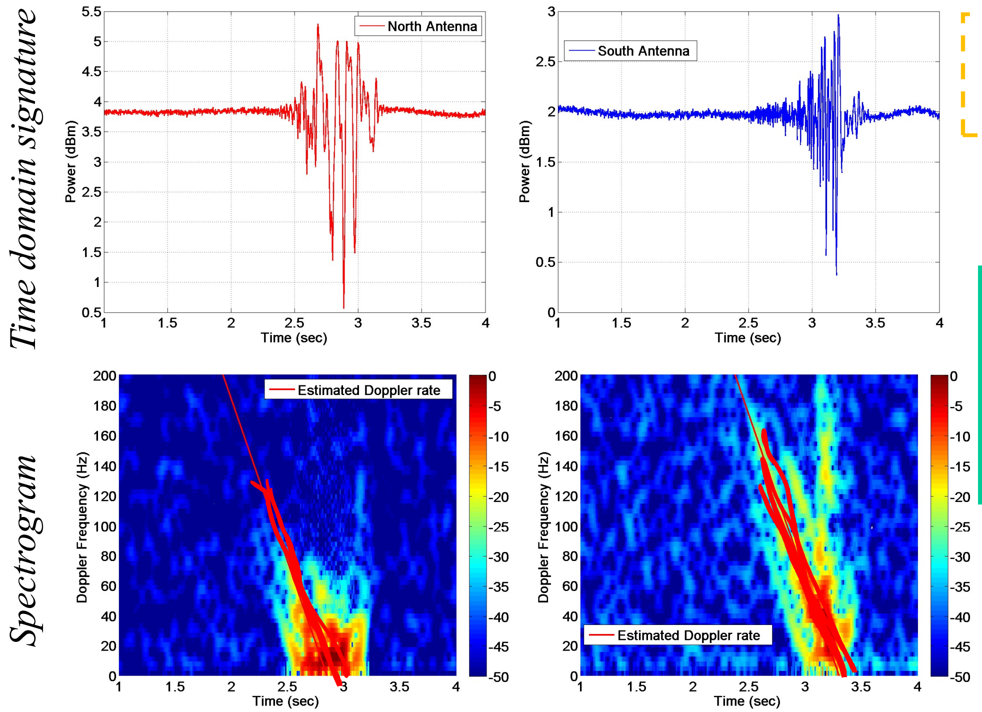

- Duration of the target signature is around 0.6 sec
  - Hamming window equal to 0.16 sec

First dataset	$\tilde{\mu}$ *(Hz/s)*	v_{ADS-B} *(m/s)*	$\tilde{v}$ *(m/s)*	*Error %*
North Antenna	214	136.2	116	20.2
South Antenna	216	136.2	116.6	19.6

✓ Acceptable agreement with the velocity provided by the ADS-B.

✓ It is noted the correspondence in terms of baseline crossing instants between the time domain signatures and the spectrograms.

✓ Only one slope is noticeable in the spectrogram due to:
- Less Doppler fluctuation as the target is in the near field of the RX
- Narrow beam of the receiving antenna, so as the target changes the altitude when approaching the 16R runway may not be within the antenna beam.

Forward Scatter Radar : FM for ATC (I)

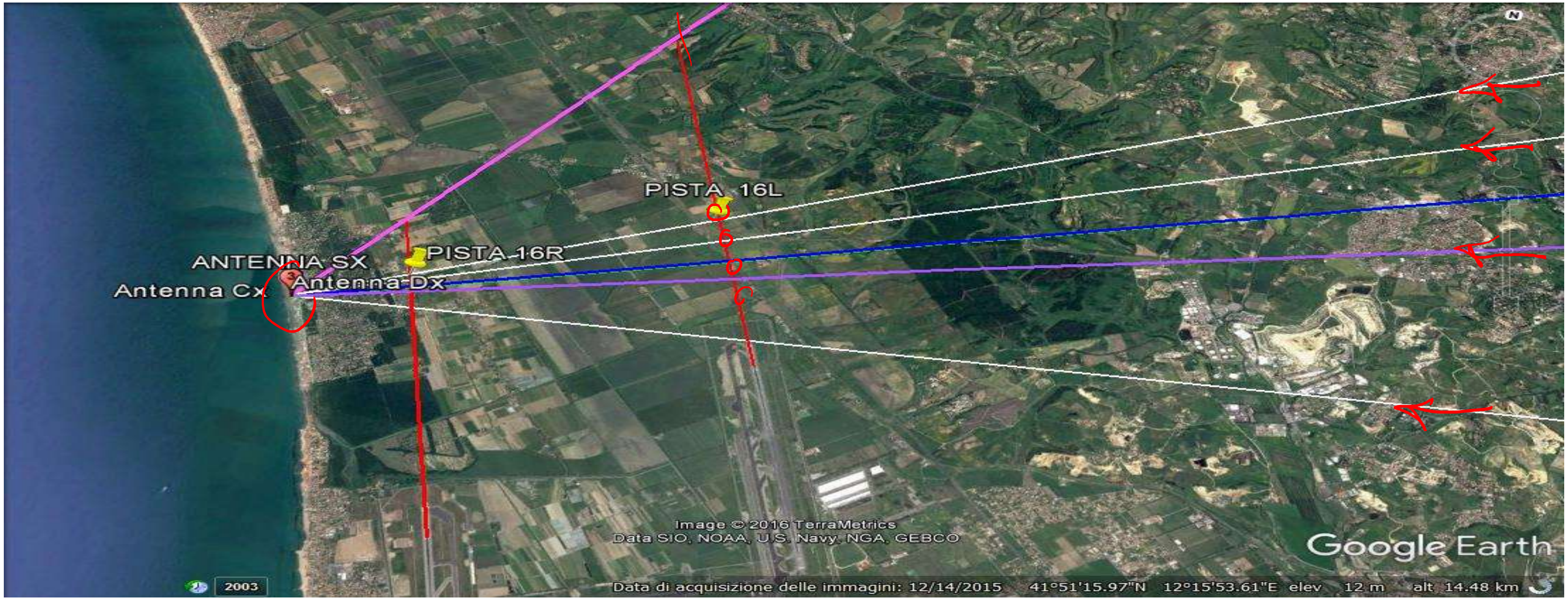

Forward Scatter Radar : FM for ATC (II)

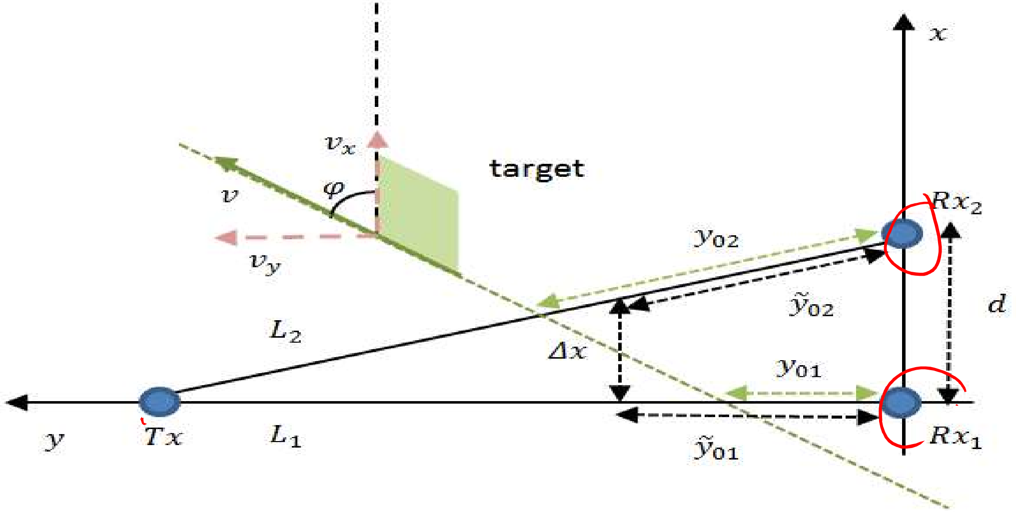

Forward Scatter Radar : FM for ATC (III)

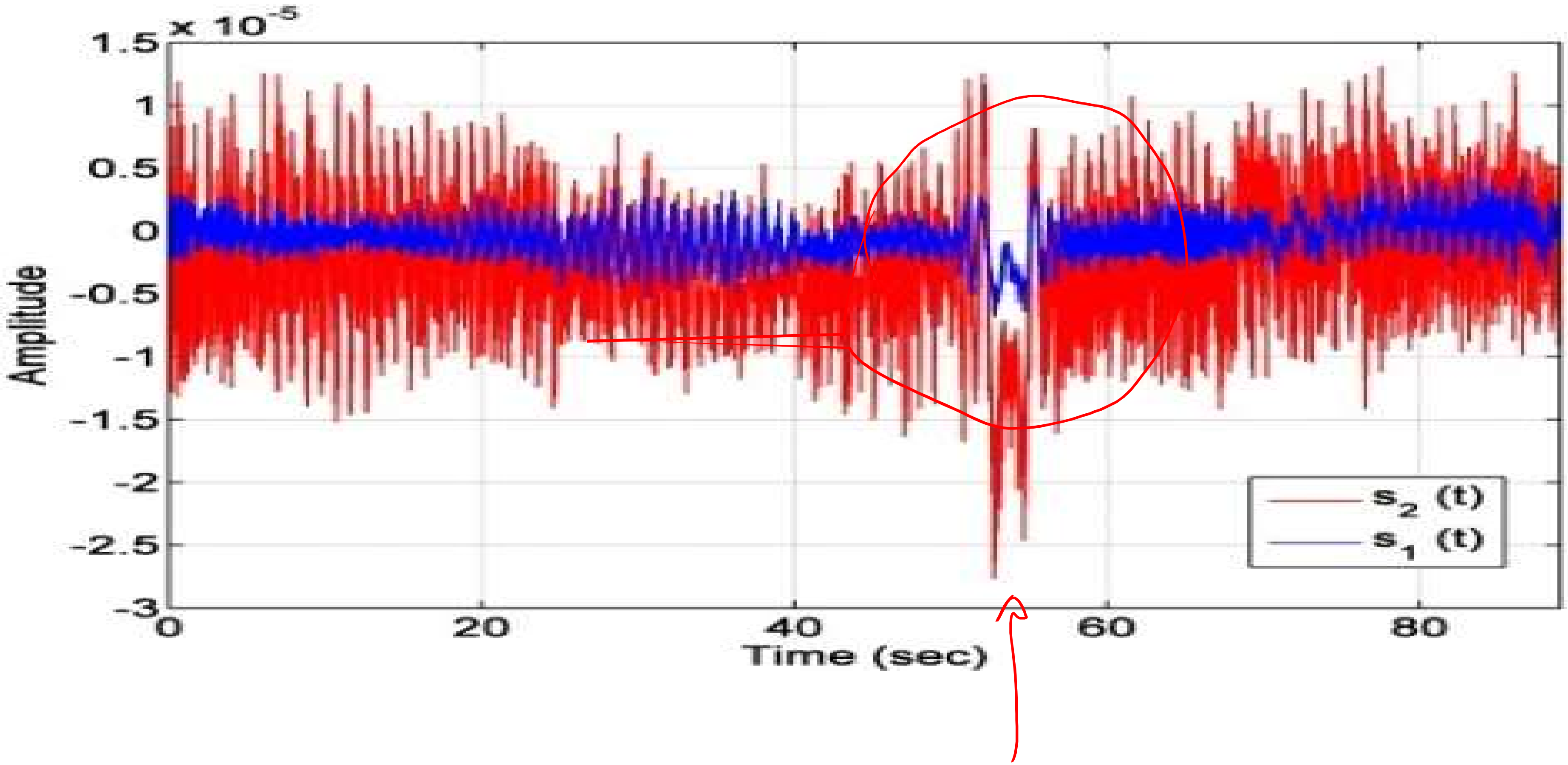

Forward Scatter Radar : FM for ATC (IV)

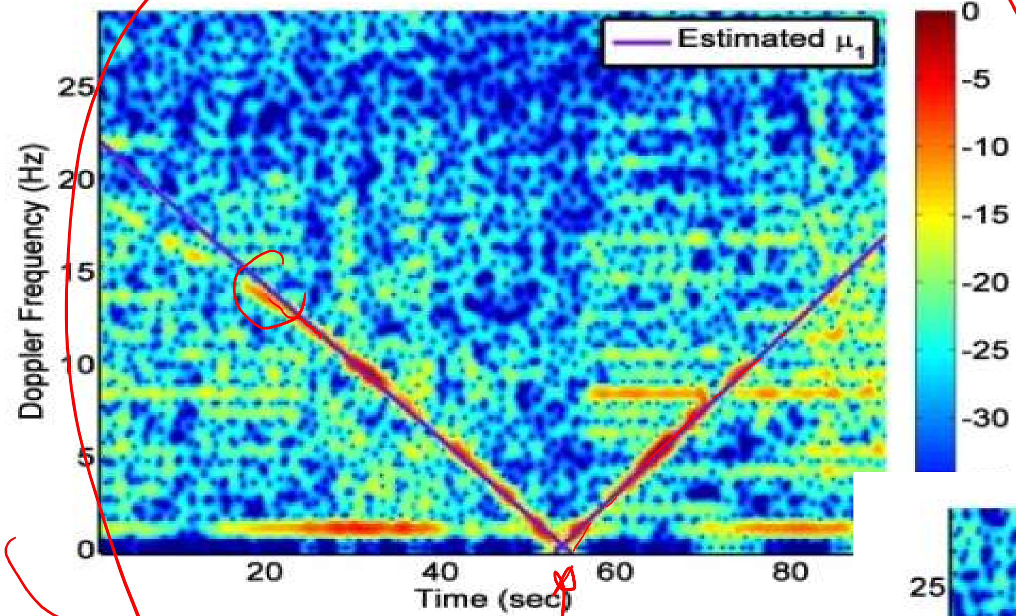

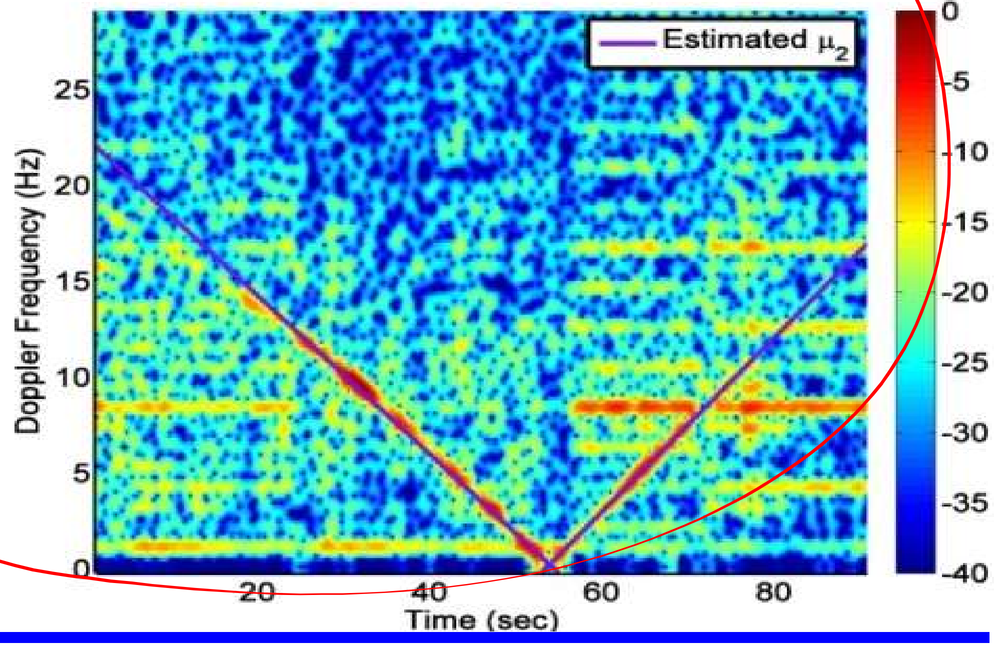

Forward Scatter Radar : FM for ATC (V)